

# The International Journal of Robotics Research

<http://ijr.sagepub.com/>

---

## **Coordinated sampling of dynamic oceanographic features with underwater vehicles and drifters**

Jnaneshwar Das, Frédéric Py, Thom Maughan, Tom O'Reilly, Monique Messié, John Ryan, Gaurav S Sukhatme and  
Kanna Rajan

*The International Journal of Robotics Research* 2012 31: 626

DOI: 10.1177/0278364912440736

The online version of this article can be found at:

<http://ijr.sagepub.com/content/31/5/626>

---

Published by:



<http://www.sagepublications.com>

On behalf of:



Multimedia Archives

**Additional services and information for *The International Journal of Robotics Research* can be found at:**

**Email Alerts:** <http://ijr.sagepub.com/cgi/alerts>

**Subscriptions:** <http://ijr.sagepub.com/subscriptions>

**Reprints:** <http://www.sagepub.com/journalsReprints.nav>

**Permissions:** <http://www.sagepub.com/journalsPermissions.nav>

**Citations:** <http://ijr.sagepub.com/content/31/5/626.refs.html>

>> [Version of Record](#) - Apr 19, 2012

[What is This?](#)

# Coordinated sampling of dynamic oceanographic features with underwater vehicles and drifters

Jnaneshwar Das<sup>1</sup>, Frédéric Py<sup>2</sup>, Thom Maughan<sup>2</sup>, Tom O'Reilly<sup>2</sup>, Monique Messié<sup>2</sup>, John Ryan<sup>2</sup>, Gaurav S Sukhatme<sup>1</sup> and Kanna Rajan<sup>2</sup>

## Abstract

*We extend existing oceanographic sampling methodologies to sample an advecting feature of interest using autonomous robotic platforms. GPS-tracked Lagrangian drifters are used to tag and track a water patch of interest with position updates provided periodically to an autonomous underwater vehicle (AUV) for surveys around the drifter as it moves with ocean currents. Autonomous sampling methods currently rely on geographic waypoint track-line surveys that are suitable for static or slowly changing features. When studying dynamic, rapidly evolving oceanographic features, such methods at best introduce error through insufficient spatial and temporal resolution, and at worst, completely miss the spatial and temporal domain of interest. We demonstrate two approaches for tracking and sampling of advecting oceanographic features. The first relies on extending static-plan AUV surveys (the current state-of-the-art) to sample advecting features. The second approach involves planning of surveys in the drifter or patch frame of reference. We derive a quantitative envelope on patch speeds that can be tracked autonomously by AUVs and drifters and show results from a multi-day off-shore field trial. The results from the trial demonstrate the applicability of our approach to long-term tracking and sampling of advecting features. Additionally, we analyze the data from the trial to identify the sources of error that affect the quality of the surveys carried out. Our work presents the first set of experiments to autonomously observe advecting oceanographic features in the open ocean.*

## Keywords

marine robotics, environmental robotics, autonomous underwater vehicles, field and service robotics

## 1. Introduction

Marine robotics has had substantial impact on the ocean sciences with the advent of mobile robotic platforms such as autonomous underwater vehicles (AUVs). These platforms have allowed oceanographers to collect data over temporal and spatial scales that would logistically be impossible or prohibitively expensive using traditional oceanographic methods involving ships and fixed moorings.

Oceanographic features are often heterogeneous and dynamic, spread over large spatial scales with dynamic biological activity across the temporal spectrum, making autonomous tracking and sampling of these features with robotic platforms challenging. For instance, biogeochemical features of interest in the coastal ocean such as phytoplankton (microscopic algae) blooms, and anoxic zones<sup>1</sup> are constantly circulated by ocean currents.

Currently, AUV-based surveys rely primarily on geographic waypoint track-line surveys (Willcox et al. 2001)

that are suitable for observing static features such as bathymetry, or slowly changing aquatic environments characterized by weak circulation (Zhang et al. 2007). When studying dynamic, rapidly evolving oceanographic features, such methods at best introduce error through insufficient spatial and temporal resolution, and at worst completely miss the spatial and temporal domain of interest. In this paper, we demonstrate methodologies for Lagrangian<sup>2</sup> observation of advecting<sup>3</sup> oceanographic

<sup>1</sup>Robotic Embedded Systems Laboratory, Department of Computer Science, University of Southern California, USA

<sup>2</sup>Monterey Bay Aquarium Research Institute, Moss Landing, USA

### Corresponding author:

Jnaneshwar Das, Robotic Embedded Systems Laboratory, Department of Computer Science, University of Southern California, Los Angeles, CA 90089, USA.

Email: jnaneshd@usc.edu

features. We describe two approaches, both utilizing GPS-tracked devices called drifters that advect with ocean currents and which have traditionally been used as proxies for advection (Lumpkin and Pazos 2007). They have been used for observation of coastal surface currents (Davis 1985) and analysis of circulation fields for improvement of ocean models (Molcard et al. 2003); usually one or more of these drifters are deployed for such studies and used in concert with ship surveys. Drifters are not generally making all, and often are making none, of the actual measurements to study biological processes. They simply become the center point for applying ship resources to study processes. We make use of drifters to **tag** patches of interest. Updates on drifter location are received periodically via tracking satellite services such as Iridium. These updates are used to plan and implement surveys that take into account the movement of the patch due to ocean currents.

This work is motivated by a multi-year inter-disciplinary field program at the Monterey Bay Aquarium Research Institute called the controlled, agile and novel observing network (CANON 2010). The program focuses on understanding rapidly evolving coastal ocean processes that have significant impacts on marine ecosystems, human health, and coastal zone economics. The initial emphasis is on phytoplankton blooms that may harm people and marine life through a variety of mechanisms (Anderson et al. 2000). Figure 1 highlights the spatio-temporal dynamics of phytoplankton blooms in Monterey bay, as observed by images acquired by a remote-sensing satellite over a period of 20 days. The drivers and biogeochemical processes behind phytoplankton bloom initiation, evolution and collapse are poorly understood in large part due to the complex interactions between the members of the microbial communities (including phytoplankton) and the surrounding environment. This necessitates acquiring measurements at sufficient spatial and temporal scales as the feature evolves.

In the past, such studies have been carried out using an array of drifters equipped with onboard sensors to observe bio-geophysical properties such as temperature, fluorescence, and salinity of advecting oceanographic features (Chavez et al. 1997). Using an array of drifters to study advecting features suffers from some operational limitations. While it is not necessarily cost-effective to deploy multiple drifters with sensors capable of measuring features of interest, some of the drifters can eventually drift in unanticipated directions due to non-coherence of ocean currents. This not only results in under-sampling of the feature, but additionally makes drifter retrieval non-trivial. Therefore, our work describes the problems and associated engineering challenges with providing the environmental context around an advecting drifter using a fully autonomous and controllable robot.

We treat our problem as a *simultaneous tracking and sampling* task, where a single GPS-tracked drifter is used to tag a patch of water providing a frame of reference along

with a survey template that is repeatedly undertaken by an autonomous platform around the advecting drifter. This methodology has certain advantages: (a) the autonomous platform can be controlled to perform a survey of a desired size and pattern and (b) the platform can be equipped with a suite of sophisticated sensors that can be exploited to sample various properties of the patch. In our work, the autonomous platform we have chosen to use is an AUV.

We demonstrate two modes of performing the surveys: (a) repeating static-plan surveys to stay with the moving patch and (b) transformed surveys carried out in the frame of reference of an advecting patch. Starting with the scientific motivation for this effort, we first lay the ground-work through analysis of past data and simulations. We derive the relationship between patch advection speed and survey dimension, and define the requirement for successful tracking in the form of an *enclosure criterion*. Subsequently we describe two field trials that demonstrate our approach. In our experiments, in addition to the sensor suite onboard the AUV, a genomic sensor is attached underneath the drifter. This allows tracking of microbial variation at the patch center along with the environmental context at the perimeter of the patch observed by the AUV.

The contribution and novelty of this work is multi-fold. First is the development of strategies to use autonomous robotic platforms for Lagrangian observations of an advecting patch and doing so in real world settings in the open ocean. Second, we show the limitations of using extensions of static surveys which repeatedly reposition a robot with the advecting patch and in the process demonstrate the importance of observation frames of reference. Third, we analytically derive an envelope on patch speeds that can be tracked autonomously. Finally, we show ways to measure the performance of such robotic surveys.

The paper is organized as follows. Section 2 places this effort in the larger context of drifter based studies, sampling and robotic control. Section 3 is the core of the paper and highlights the technical approach we follow. Section 4 shows the experimental setup in the field. Section 5 analyzes a five-day field experiment conducted in September 2010 in the open ocean followed by conclusions and some future work in Section 6.

## 2. Related work

Drifters have traditionally been used for Lagrangian studies for measurement of biological processes in situ at the appropriate temporal scales with ship-support (Chavez et al. 1997), and for physical oceanographic measurements of current flow and turbulence related to ocean modeling (Molcard et al. 2003; Salman et al. 2008). Our work extends these applications from a pure drifter-based Lagrangian observation system to one which provides a larger environmental context as well as more control of the survey design using an autonomous robotic platform.

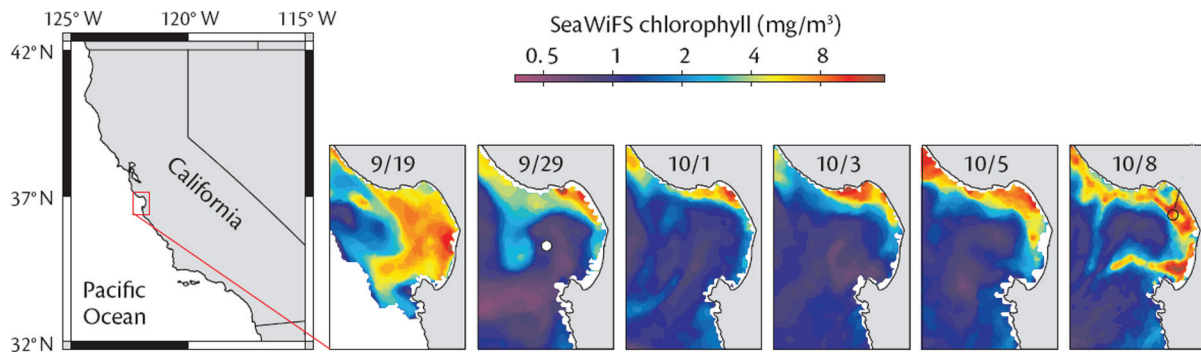


**Fig. 1.** Dynamics of algal blooms in California's Monterey Bay. Figure shows remote sensing images capturing the chlorophyll concentration at the ocean surface between September 19th and October 8th, 2002. Due to atmospheric conditions, the images are temporally aperiodic. Algal hotspots characterized by red coloration can be seen evolving as a result of biological growth and decay, and advection due to ocean currents. Marine scientists are interested in understanding the dynamics of these hotspots as they evolve, which necessitates being able to track them spatially as they are advected by ocean currents, and sampling within this patch frame of reference. (Reproduced with permission from (Ryan et al. 2005).)

Tracking of oceanographic features with AUVs has previously been addressed with the help of ocean models. Advection forecasts provided by regional ocean models in the form of virtual drifters have been used for planning trajectories for gliders to track the boundary and centroid of a patch of water (Smith et al., 2010b, Smith et al., 2010a). However, glider trajectories computed for virtual drifters are not guaranteed to track a physical patch of water since such model forecasts suffer from high uncertainty. Further, the work is limited by the speed and motion of gliders which are highly restrictive and influenced by currents which have resulted in focused demonstration of boundary and centroid tracking. In contrast, the goal of this work is to track a patch and sample within it rapidly.

Tracking and rendezvous with moving targets has been covered in the robotics literature, although the focus has been on interception and entrapment with multiple robots (Mas et al. 2009), rather than sampling in the target frame-of-reference. Saripalli and Sukhatme (2003) demonstrated landing of an unmanned aerial vehicle on a moving target. Frew and Lawrence (2005) demonstrated control strategies wherein a team of autonomous aircraft orbit a moving target while maintaining a specified distance (standoff line-of-sight tracking). Franchi et al. (2010) used a terrestrial multi-robot system using low-level control to localize and encircle a moving target in a lab environment. In the ocean sciences, Hu et al. (2011) discuss the use of drifters for tracking anticyclonic eddies in near coastal waters; however, they use a Lagrangian frame of reference to navigate their manned support vessel.

Feature tracking with AUVs has been discussed in the context of multiple gliders in the Monterey Bay by Fiorelli et al. (2006), while coordinated sampling with a fleet of gliders is demonstrated in Zhang et al. (2007). A methodology for iceberg relative-terrain-aided navigation has been proposed for AUVs using sideways looking sonar maps

generated by a ship (Kimball and Rock 2010). However, the authors abstract the iceberg deformation and its motion while relying on the closed structure of a solid body.

Our work is distinct in that environmental observation and sampling drive the survey methodology using onboard planning techniques within the oceanographic domain. More importantly the focus of this work is on deriving the frames of reference for undertaking such observations which none of the prior work addresses. To the best of our knowledge, our work presents the first study where an autonomous robot samples in the Lagrangian frame of reference of an advecting oceanographic feature in the upper water-column.

### 3. Technical approach

AUVs are equipped with scientific payloads to enable sampling of bio-geochemical properties of interest at desired sampling rates. Typically while sampling the upper water-column, track-line based surveys are carried out. A prominent example is the 'radiator' or 'lawnmower' pattern shown in Figure 2. It shows an aggregation of phytoplankton, identified by the fluorescence of their chlorophyll during daytime operations when biological activity is concentrated in the upper portions of the shelf in Monterey Bay. The vertical saw-tooth profiling path of the AUV illustrated in this figure is called a 'yo-yo' and allows observation of a three-dimensional snapshot of the water-column. The patterns are usually determined a priori according to scientific need.

Existing AUV sampling methodologies use survey patterns designed in the Earth frame, i.e. they are not planned and carried out relative to the water mass. Hence, by design, these *static-plan surveys* are suitable for features that do not

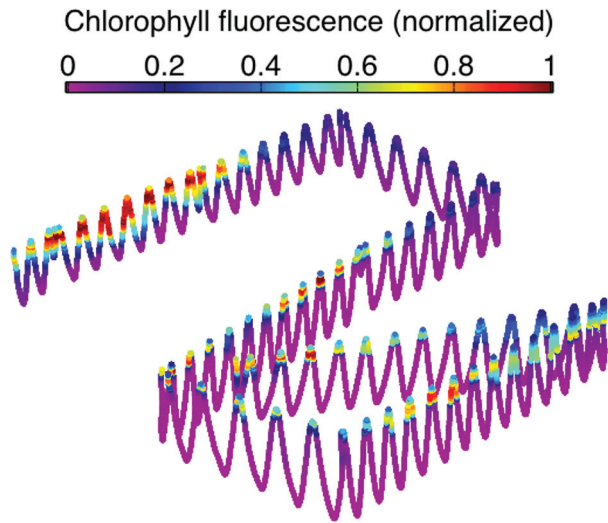


**Fig. 2.** A lawnmower survey pattern of an AUV in the upper water-column showing chlorophyll fluorescence within vertical saw-tooth (or ‘yo-yo’) profiles.

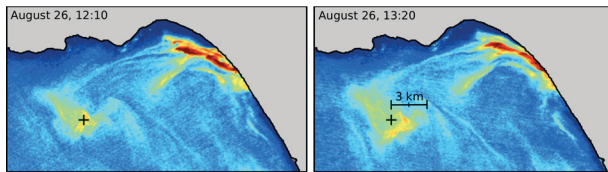


**Fig. 3.** Airborne remote sensing images showing short-term phytoplankton bloom dynamics in the Monterey Bay in the month of August 2009. A phytoplankton bloom patch, marked in the left image with a +, is shown advecting eastward by ~1 km in less than 70 min, suggesting currents of the order of ~0.2 m/s.

move out of the survey’s region of coverage or are sufficiently slow for an AUV with typical speeds of ~1.5 m/s to resolve adequately. The oceanographic features of interest in our study, however are not static; movement occurs either due to surface currents, the geography of the coastal shelf, wind-driven conditions or all of the above. Figure 3 shows remote sensing imagery of chlorophyll concentration in the upper 5–10 m of Monterey bay. The hotspots (regions with warm colors) were advected at ~1 km/h.

The scientific goal of this work is to extend existing oceanographic sampling methodologies to perform Lagrangian observation studies to sample such advecting features of interest. We approach this problem in two ways:

**Track a patch:** we use GPS-tracked Lagrangian drifters, used as proxies for advection by marine scientists, to tag an identified patch of interest;

**Sample the patch:** we extend existing oceanographic survey patterns to sample within the context of the advecting water patch tagged by the drifter. Frequent position updates

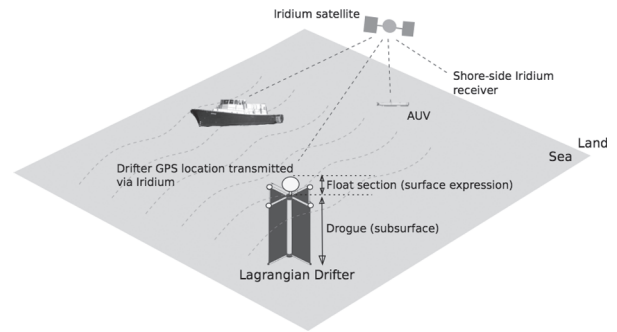


**Fig. 4.** Illustration of a Lagrangian drifter being tracked on shore and at sea. The drifter has a float section affected mostly by wind and a drogue section which is impacted by sub-surface currents. Drifter locations are transmitted via satellite. The support vessel is for launch, recovery and charging of the AUV.

from the drifter are used to estimate the short-term trajectory of the patch, and two approaches are demonstrated to stay with the patch and sample around or within it.

### 3.1. Tracking advecting patches

We use GPS-tracked drifters to tag the center of an advecting water patch. These patches are usually identified by using data from remote-sensing satellites, pilot AUV static-plan surveys, and ship-board measurements. Once detected, a bloom center is marked with a GPS-tracked drifter and position updates are obtained from the drifter at regular intervals of ~2 min via a satellite communication network such as Iridium. To improve the drifter’s signature of patch advection, which may experience a range of sub-surface currents, drogues are often used to improve the surface and sub-surface expression for advection. Figure 4 illustrates the usage of a GPS-tracked Lagrangian drifter and its communication channels with shore, ship, and AUV.

### 3.2. Scientific motivation

Two primary science goals drive our work; resolving the boundary of a patch, and the interior of a patch. The first goal requires a survey template that repeatedly circumscribes the volume boundary such as a box pattern shown in Figure 5. The second goal is to map the interior of the volume in order to understand the biological dynamics occurring within the volume of the patch, requiring a template that passes through the volume interior such as in the lawnmower pattern described earlier. Both goals are relevant to the overarching research objective to understand the environmental factors influencing the growth and ecology of phytoplankton communities. The box pattern was chosen for our open-ocean field experiment, although the results can be generalized to other patterns.

Our work extends existing static-plan surveys to the observation of advecting features of interest. To achieve this

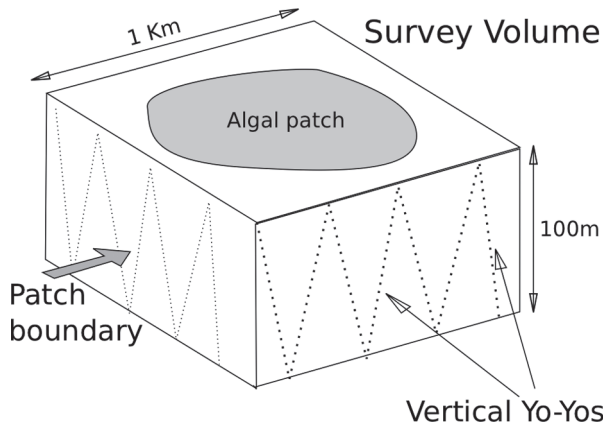


**Fig. 5.** The box survey pattern of an AUV which circumscribes a patch volume being sampled.

goal, we first tag an identified patch of interest with a GPS-tracked drifter. The decision of where and when to tag a water patch is usually driven by a combination of oceanographic conditions such as wind, real-time surface currents, geographical conditions, historical data and remote sensing information when available. A specific assumption we make is that the AUV does not compute currents for executing the survey around the drifter primarily for two reasons. In situ determination of current velocities using an acoustic Doppler current profiler (ADCP) is challenging given integration times and signal noise from this sensor. Second, drifter speed and bearing are computed shore-side and transmitted to the vehicle providing adequate information for the vehicle's onboard planner to generate a plan to meet the coverage goal of the experiment.

Based on the scientific motivation above, our problem statement is as follows:

**Problem statement:** Extend existing oceanographic surveys by an autonomous platform to observe an advecting water patch of interest, such that the patch-center tagged by a GPS-tracked drifter remains within the survey perimeter at all times.

### 3.3. Lagrangian survey design

AUV surveys are characterized by the pattern in the horizontal plane (e.g. lawnmower, box, etc.), the pitch angle for the yo-yos and a depth-envelope specifying the maximum and minimum depths. For the purpose of planning, we approximate the motion of the AUV to the horizontal plane by projecting its velocity by the pitch angle. Figure 6 shows a box pattern that has a square profile in the horizontal plane with edge length  $l$ . The vertical saw-tooth pattern with pitch angle  $\theta$  allows the AUV to sample the vertical faces of a cube which is essential for the patch boundary study. In the following discussion, we use this pattern as the

template for analysis and design of our approach for the two modes. We begin by defining terms used in our design:

**Earth frame:** the geographic frame of reference which allows the specification of every location on Earth uniquely. Typically static-plan AUV surveys are planned in the Earth frame in the form of track waypoints using a longitude/latitude-based spherical coordinate system.

**Drifter frame:** the frame of reference relative to the advecting patch. Since the patch is tagged by a GPS-tracked drifter we set the origin of the patch frame to the drifter location and orient it to point along the direction of drifter advection.

**Repeated static-plan surveys:** these are static-plan surveys carried out repeatedly by catching up with the drifter after each iteration. Survey patterns are intended for **Earth frame**, but we do our analysis by visualizing these in the **drifter frame**.

**Trailing distance:** to perform repeated static-plan surveys, the AUV needs to catch-up with the last observed location of the drifter on completion of the current static-plan iteration. The distance the AUV lags or trails behind its survey *start location* for the next iteration is called the *trailing distance*.

**Transformed surveys:** in contrast to repeated static-plan surveys that are designed in the Earth frame, these patterns are designed relative to the patch frame or the **drifter frame**. Since the AUV operates in the Earth frame, this entails transformations between the advecting drifter frame and the Earth frame.

**Enclosure criterion:** ideally the drifter should remain within the perimeter of the pattern while the AUV is executing the pattern. The *enclosure criterion* ensures that the AUV encapsulates and characterizes the volume by enforcing the constraint that the patch center marked by the drifter always stays within the perimeter of the survey. Figure 7 shows the limiting condition for the enclosure criterion for repeated static-plan surveys with a box pattern. In Section 3.3, we obtain the bounds on drifter speed for the satisfaction of the enclosure criterion for repeated static-plan surveys; transformed surveys by definition ensure satisfaction of the enclosure criterion.

We have identified two ways of approaching our goal to perform Lagrangian observation studies: (a) repeated static-plan surveys and (b) transformed surveys. In repeated static-plan surveys, we perform existing oceanographic surveys repetitively, repositioning the AUV to the latest location of the drifter once a survey or iteration is complete. In the case of transformed surveys, we *design the pattern in the drifter frame* and transform it back to the Earth frame to obtain the plan to command the AUV. To plan the surveys in

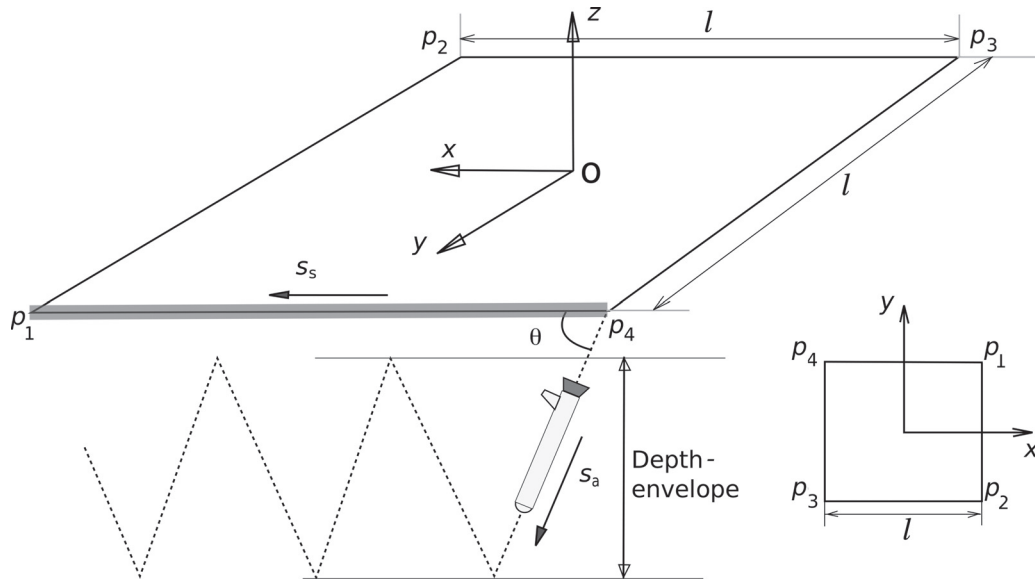


**Fig. 6.** Illustration of the box survey pattern. For a box pattern with edge length  $l$ , implemented in three dimension, the AUV performs saw-tooth vertical profiles along the edges with pitch angle  $\theta$ . The AUV moves at a constant surge speed  $s_a$ . The projected speed of the AUV on the horizontal plane while executing the saw-tooth profiles is given by  $s_a \cos \theta$ . We can design AUV plans in two-dimensions where the motion along the depth axis is encapsulated by the projection onto the horizontal plane.

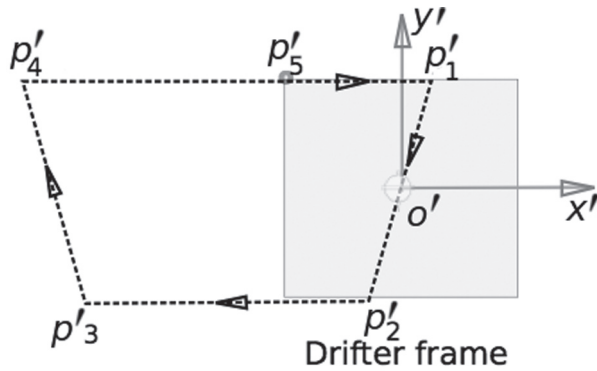


**Fig. 7.** Enclosure criterion satisfied in drifter frame. The goal of our study is to implement surveys such that a drifter that represents a patch of water stays within the boundary of the survey. In the figure,  $p'_1 \dots p'_5$  defines the perimeter of a survey in the drifter frame. The enclosure criterion ensures that the drifter, marked by  $o'$ , stays inside the survey perimeter.

both repeated static-plan surveys and transformed surveys, we require an estimate of the drifter path in the near-term ( $\sim 2$  h).

**3.3.1. Repeated static-plan surveys** Repeated static-plan surveys are planned in the Earth frame with respect to the current location of the drifter. Once the survey is complete, the latest drifter location is obtained and the AUV traverses to the new survey location and carries out another survey. We define this as a survey iteration. Repeated iterations are carried out till the mission is over, or the drifter moves out of an area of interest. We derive the maximum drifter speed for which static-plan surveys satisfy the enclosure criterion.

Consider an AUV that is required to perform a static-plan box pattern around a drifter that is moving with a speed of  $s_d$ . We will consider a simple scenario where at the beginning of the  $n$ th iteration of the experiment, the drifter is moving in a straight line and the AUV is at a trailing distance of  $u_n$  from the initial waypoint of the static-plan survey relative to the drifter's current location.

Let the surge speed of the AUV be  $s_a$  performing a straight line transect and the speed during the survey when it is performing a saw-tooth pattern with a pitch angle  $\theta$  be  $s_s$ , where  $s_s = s_a \cos \theta$ . For our analysis, we assume that the AUV is lagging directly behind the drifter and for illustrative purposes, we will use a box pattern with edge length  $l$ . The total distance the AUV needs to travel as viewed on the horizontal plane is given by the sum of trailing distance  $u$ , and the survey length for the box pattern  $L_{\text{survey}}$ . For the box pattern,  $L_{\text{survey}} = 4l$ . Given  $u_n$ , the trailing distance for the  $n$ th survey iteration of an experiment, we first show that within a few survey iterations, the trailing distance converges to  $u^*$ . The total time taken by the AUV to complete the survey is given by

$$T_s = \frac{u_n}{s_a} + \frac{L_{\text{survey}}}{s_s} \tag{1}$$

where  $\frac{u_n}{s_a}$  is the time taken for the AUV to reach the starting point at the AUV surge speed  $s_a$ . Once the starting point has been reached, the AUV initiates the yo-yos, resulting in the projected speed of  $s_s$ . The time taken for completion of the survey is given by the second term  $\frac{L_{\text{survey}}}{s_s}$ .

The trailing distance for the  $n + 1$ th iteration is the distance the drifter travels while the AUV finishes the  $n$ th survey. For the  $n + 1$ th iteration, the AUV hence lags or

trails behind the starting waypoint for the iteration by this distance given by

$$u_{n+1} = T_s s_d. \tag{2}$$

Substituting  $T_s$  from Equation (1) to Equation (2) we get

$$u_{n+1} = \left[ \frac{u_n}{s_a} + \frac{L_{\text{survey}}}{s_s} \right] s_d. \tag{3}$$

Using  $a = \frac{s_d}{s_a}$  and  $b = L_{\text{survey}} \frac{s_d}{s_s}$  in Equation (8), we get

$$\begin{aligned} u_{n+1} &= u_n \frac{s_d}{s_a} + L_{\text{survey}} \frac{s_d}{s_s} \\ &= a u_n + b \\ &= a(a u_{n-1} + b) + b \\ &= a^3 u_{n-2} + b(1 + a + a^2). \end{aligned}$$

The trailing distance for the  $n + 1$ th iteration is hence of the form

$$u_{n+1} = a^i u_{n-i+1} + b \sum_{k=0}^{i-1} a^k, \tag{4}$$

where  $0 \leq i \leq n + 1$ . On putting  $i = n + 1$  in the above equation, we get

$$u_{n+1} = a^{n+1} u_0 + b \sum_{k=0}^n a^k. \tag{5}$$

In the limit, where  $n \rightarrow \infty$ , Equation (5) gives us the asymptotic trailing distance  $u^*$

$$u^* = u_0 \lim_{n \rightarrow \infty} a^{n+1} + b \lim_{n \rightarrow \infty} \sum_{k=0}^n a^k. \tag{6}$$

But  $a < 1$  for  $s_d < s_a$ , hence

$$u^* = b \sum_{k=0}^{\infty} a^k.$$

For  $a < 1$ ,  $\sum_{k=0}^{\infty} a^k = \frac{1}{1-a}$

$$u^* = \frac{b}{1-a}. \tag{7}$$

Substituting values of  $a$  and  $b$

$$u^* = \frac{L_{\text{survey}} s_a s_d}{s_s (s_a - s_d)}. \tag{8}$$

Hence, for survey length  $L_{\text{survey}}$ , AUV surge speed  $s_a$ , drifter speed  $s_d < s_a$ , and pitch-angle  $\theta$ , the trailing distance converges asymptotically to  $u^* = \frac{L_{\text{survey}} s_d}{\cos \theta (s_a - s_d)}$ . The asymptotic trailing distance is hence independent of the initial trailing distance  $u_0$  and depends only on the drifter speed  $s_d$ . Note that the maximum drifter speed observed in historic drifter data is 0.6 m/s, about half of the maximum AUV surge speed of 1.5 m/s.

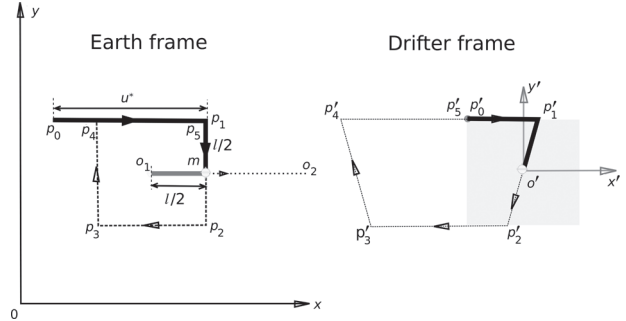


**Fig. 8.** Implementation of the box pattern for Lagrangian observation studies involves the AUV covering a trailing distance  $u$ , the survey length  $4l$  and ensuring that the enclosure criterion is satisfied.  $o_1$  represents the starting point of the drifter and  $o_2$  its termination within a single pattern. For the enclosure criterion to be satisfied, the AUV has to cross the drifter ahead of its path in the Earth frame.

We use the above result to determine the maximum drifter speed for which the enclosure criterion is satisfied in the drifter frame. For the enclosure criterion to be satisfied, the AUV has to cross the drifter ahead of its path in the Earth frame, as illustrated in Figure 8. Hence, for the box pattern with edge length  $l$ , the drifter must travel less than  $l/2$  in the time the AUV takes to intercept the drifter:

$$\left[ \frac{u^*}{s_a} + \frac{l/2}{s_s} \right] s_d < l/2 \tag{9}$$

$$\frac{u^*}{s_a} + \frac{l}{2s_s} < l/2s_d. \tag{10}$$

Using Equation (8) with  $L_{\text{survey}} = 4l$  and solving for  $s_d$

$$s_d < \frac{s_a(1 + 30 \cos \theta + \cos^2 \theta)^{1/2} - s_a(1 - \cos \theta)}{14}. \tag{11}$$

For  $s_a = 1.5$  m/s,  $\theta = \pi/8$ , Equation (11) results in  $s_d < 0.36$  m/s. This sets the **upper bound** on the drifter speed for which we can successfully complete repeated static-plan surveys while satisfying the enclosure criterion in the **drifter** frame. We obtained drifter logs from a deployment in Monterey Bay during August 2006 lasting 18 days (STELLA 2006). From this dataset, we utilized a 3.5 day section during which the drifter traveled a total of 80 km near Monterey Bay as shown in Figure 9.

The computed distribution of drifter speeds observed during this period for use in our analysis is shown in Figure 10. The dotted line in this figure marks this upper-bound of 0.36 m/s for which the enclosure criterion is satisfied. As highlighted by the cumulative frequency curve in Figure 10, for 30% of the speeds the vehicle would not be able to satisfy the enclosure criterion. This poses a limitation in the use of repeated static-plan surveys for Lagrangian observation studies, since it cannot be guaranteed that the drifter stays within the perimeter of the survey at all times. To address this limitation, we present an alternative approach

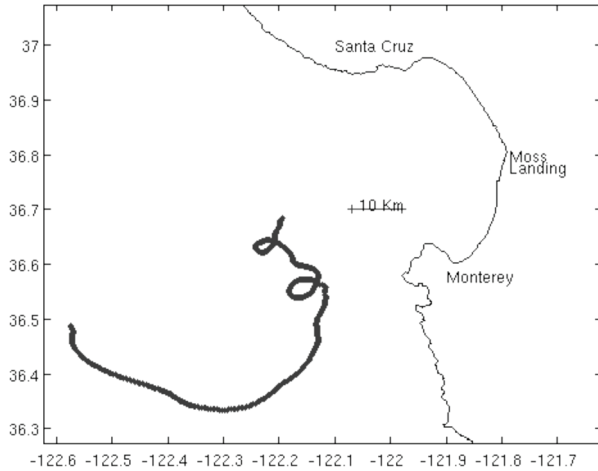


**Fig. 9.** Trajectory of a drifter advected in the vicinity of Monterey Bay in August 2006 for a period of 3.5 days.

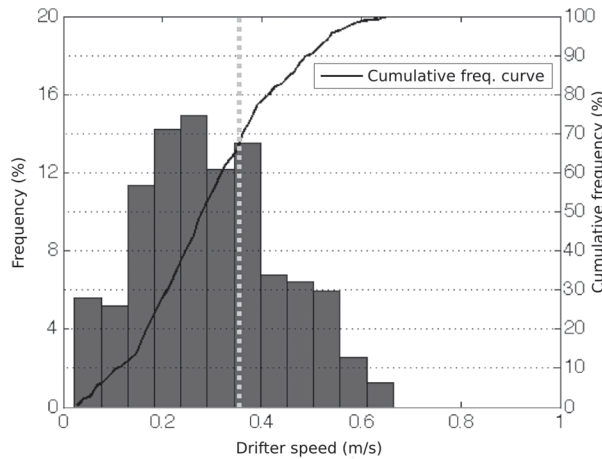


**Fig. 10.** Distribution of speeds for a drifter deployed at the central Californian coast. The dotted line shows the upper-bound of 0.36 m/s on drifter speed for which the enclosure criterion is satisfied. This is based on our analysis of repeated static-plan box surveys performed by an AUV operating at nominal speed of 1.5 m/s.

in the following discussion that by design ensures that the enclosure criterion is satisfied for a wider range of drifter speeds.

**3.3.2. Transformed surveys** Instead of repeating static-plan surveys planned in the Earth frame of reference based on periodic updates of patch trajectory, we can design the surveys in the drifter frame of reference. We call these *transformed surveys* since the waypoints of the surveys are planned in the drifter frame of reference and then transformed back to the Earth frame. As opposed to repeated static-plan surveys where we observed an upper-bound of 0.36 m/s, transformed surveys by design ensure that the enclosure criterion is satisfied. The key idea is as follows.

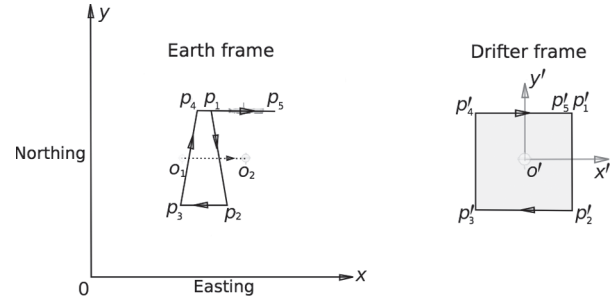


**Fig. 11.** Illustration of transformed survey for the box pattern. The goal is to ensure that a box pattern is implemented in the advecting drifter frame of reference. The goal waypoints for the corners of the box pattern in the drifter frame are transformed to the Earth frame to provide us with the AUV mission plan consisting of five waypoints.

Given a desired survey pattern, for example a ‘lawn-mower’ or a ‘box’, we acquire the frame of reference of the advecting water patch from the GPS-tagged drifter. Since AUVs are commanded using waypoints in the Earth frame, we want to plan waypoints and AUV operation parameters (speed, pitch angle), which will result in the desired survey being executed in the drifter frame of reference. Hence, this approach requires transformations between the advecting drifter frame of reference and the static Earth frame. Figure 11 illustrates the transformation between Earth and drifter frame for the box pattern.

There are two ways of implementing transformed surveys. The first is to perform a survey at a constant speed *in the drifter frame*. However, we will show that due to the transformations between the advecting drifter frame and the static Earth frame, such surveys require the AUV to travel in the Earth frame at variable speeds. To simplify, command and control and to utilize the maximum AUV speed *at all times* (in the previous case, the maximum AUV speed is utilized only for sections of the survey), we describe a second approach that involves running the AUV at a constant speed (ideally the maximum operational speed of the AUV). This however results in a survey pattern in the drifter frame with variable speed. We discuss both the cases below, and show experimental results for the latter in Section 4.

**Constant AUV speed in the drifter frame:** one goal is to perform the template at constant speed relative to the drifter, ensuring uniform sampling rate in the drifter frame. In Figure 12, we show a box pattern with five corner waypoints forming the complete survey. Given the desired speed at which we want the AUV to sample relative to the drifter and the length of the survey, the corner waypoints are denoted by  $p'_i = [x'_i, y'_i, 1]^T$ . Additionally, since the AUV appears to travel at constant speed in the drifter frame, we can compute the time  $t_i$  when the AUV should be at each waypoint. If  $\phi$  is the angle between the drifter frame and the Earth frame and the drifter is at  $o_i$  at each time-step  $t_i$ , we can construct the homogeneous transformation matrix (Sciavicco et al. 2000)

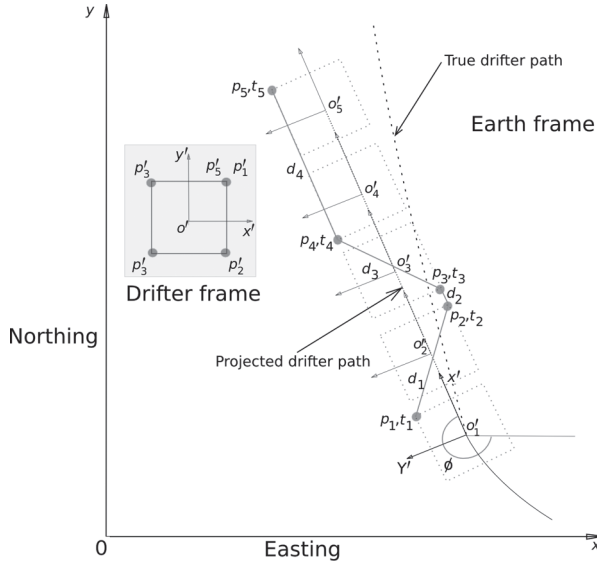


**Fig. 12.** Illustration of a transformed survey for the box pattern for the case where the AUV is required to move at constant speed in the drifter frame. Given the five goal waypoints and the corresponding time of arrival  $(p'_1, t'_1), \dots, (p'_5, t'_5)$  for the corners of the box pattern, our goal is to compute  $(p_1, t_1), \dots, (p_5, t_5)$ . For this computation, we require a prediction of the drifter trajectory for the duration of the iteration. This is done using a linear projection of the drifter trajectory based on the last two position updates from the drifter. For the box pattern, the AUV will travel varying distances  $d_1, d_2$  and  $d_4$  in the Earth frame, for equal time intervals corresponding to each leg of the survey.

$H_w^d$  that transforms the waypoints in the drifter frame to the Earth frame, given by

$$H_w^d = \begin{bmatrix} \cos \phi & -\sin \phi & o_{ix} \\ \sin \phi & \cos \phi & o_{iy} \\ 0 & 0 & 1 \end{bmatrix}. \tag{12}$$

Given  $p'_i$ , a coordinate in drifter frame, the corresponding coordinate in the Earth frame can then be given by

$$p_i = H_w^d p'_i. \tag{13}$$

Given the current AUV coordinate in the Earth frame and the destination computed using Equation (13), we can then compute the required projected AUV speed to achieve the target in the drifter frame at the desired time instant. As illustrated in Figure 12, the AUV needs to travel varying distances  $d_1, d_2$  and  $d_4$  in the Earth frame, for equal time intervals for each leg of the box pattern. Consequently, the maximum required projected AUV speed in the Earth frame constrains the maximum speed at which sampling can be done in the drifter frame of reference.

**Constant AUV speed in the Earth frame:** in the case of transformed surveys with constant AUV speed in the drifter frame, we observe that the optimal AUV speed is not utilized for the duration of the survey. Depending on their power consumption, every AUV has an optimal speed that

allows the vehicle to cover a maximum distance on a single survey (Bellingham and Willcox 1996). In the case of the Dorado AUV used in our experiments, this speed is  $\sim 1.5$  m/s for a total mission duration of 18 h on a single charge. For this reason we consider the case where we want the AUV to move at a **constant speed in the Earth frame**.

Given the initial AUV coordinate, initial drifter coordinate, latest drifter velocity, AUV pitch angle and commanded AUV speed we need to compute the required AUV trajectory in the Earth frame. As shown in Figure 13(b), let  $o$  represent origin of the Earth frame. Let  $o'$  and  $o''$  represent the origins of the initial and final drifter frames, also representing the coordinates of the drifters. Let the initial location of the AUV be  $p_1$ . Given a goal of  $p'_2$  in the drifter frame, we want to compute  $p_2$ , i.e. the AUV coordinate in the Earth frame.

We start with the observation that the time taken by the AUV to travel from  $p_1$  to  $p_2$  in the Earth frame is equal to the time taken for the drifter to advect from  $o'$  to  $o''$ . Hence

$$\frac{|p_1 - p_2|}{s_a} = \frac{|o'' - o'|}{s_d}. \tag{14}$$

The goal waypoint in the Earth frame,  $p_2$ , can be obtained by transforming  $p'_2$  from the drifter frame to the Earth frame. This is given by

$$p_2 = p'_2 H_o^{o''} \tag{15}$$

where  $H_o^{o''}$  is the homogeneous transform defined by

$$H_o^{o''} = \begin{bmatrix} \cos(\phi - \pi/2) & -\sin(\phi - \pi/2) & o''_x \\ \sin(\phi - \pi/2) & \cos(\phi - \pi/2) & o''_y \\ 0 & 0 & 1 \end{bmatrix}. \tag{16}$$

Equation (14) then becomes

$$\frac{|p_1 - p'_2 H_o^{o''}|}{s_a} = \frac{|o'' - o'|}{s_d}. \tag{17}$$

On solving Equation (17), we obtain the final drifter coordinate  $o''$ . Using the solution for  $o''$  in Equation (15), we compute the final goal of the AUV in the Earth frame for the given target  $p'_2$  in the drifter frame. Given the current velocity of the drifter  $s_d$ , the goal is to compute waypoints to implement the survey pattern in the drifter frame, assuming linear motion of the drifter. Figure 14 illustrates an iteration of the experiment, where the initial position of the drifter is  $d_1$  at time  $t_1$ . Subsequently a survey plan using the waypoints  $p_1 \dots p_5$  is computed in the Earth frame with arrival times of  $t_1 \dots t_5$ .

### 3.4. Repeated static-plan surveys versus transformed surveys

Having computed the upper bounds on drifter speed for repeated static-plan surveys and having formulated the approach for transformed surveys, we now compare the two approaches in simulation. We will start by defining two metrics that will allow us to compare the performance of each

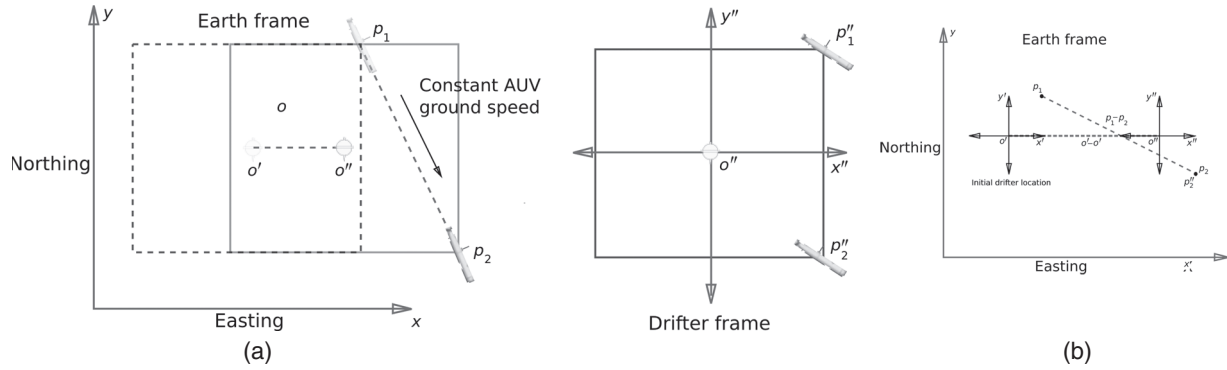


**Fig. 13.** Illustration of survey planning with constant AUV speed in the Earth frame: (a) illustration of AUV navigation between two waypoints of the box pattern using constant speed in Earth frame. As the drifter moves from  $o'$  to  $o''$ , the AUV moves at constant ground speed from  $p_1$  to  $p_2$ . This results in the AUV moving from  $p_1''$  to  $p_2''$  in the drifter frame. Given the drifter speed  $s_d$ , the initial AUV location  $p$  and the goal location of the AUV in drifter frame,  $p_2''$ , we need to compute the corresponding goal location in the Earth frame,  $p_2$ ; (b) computation of AUV target waypoints for transformed survey with constant AUV speed in the Earth frame. Given an initial AUV location in the Earth frame,  $p_1$ , the goal is to compute the waypoint  $p_2$  in the Earth frame that corresponds to a desired coordinate in the drifter frame,  $q''$ .

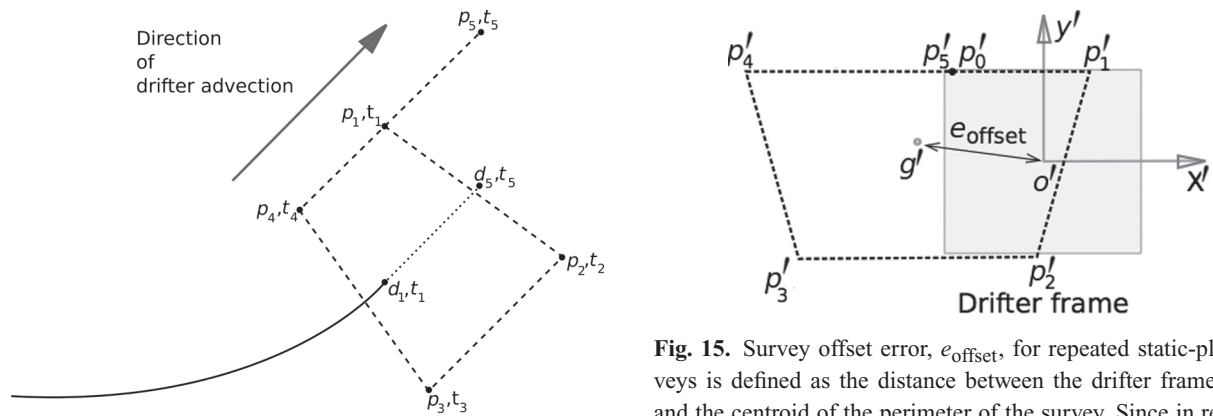


**Fig. 14.** An illustration of an iteration of a transformed box survey with constant AUV ground speed in the Earth frame. Based on previously observed drifter positions, a linear projection of the drifter trajectory is computed for the duration of the iteration. In this figure, we assume the AUV is already at the initial waypoint  $p_1$  at time  $t_1$  which corresponds to the first-corner waypoint of the box pattern in the drifter frame. We know the desired waypoints for the other corners of the box pattern,  $p_2'' \dots p_5''$ . Using the solution to Equation (17), we obtain the locations and times of the other four waypoints, giving us the complete plan for the iteration,  $(p_1, t_1) \dots (p_5, t_5)$ .

approach: (a) *survey offset error* and (b) *survey time*. We define the survey offset error as the distance between the drifter and the center of the survey in the drifter frame. This metric will be used as a measure of how well our approach performs for various drifter speeds. As illustrated in Figure 15, if  $o'$  is the drifter frame origin and  $g'$  is the centroid of the perimeter of the survey in the drifter frame, then the offset error is defined by

$$e_{\text{offset}} = |o' - g'|. \tag{18}$$

**Fig. 15.** Survey offset error,  $e_{\text{offset}}$ , for repeated static-plan surveys is defined as the distance between the drifter frame origin and the centroid of the perimeter of the survey. Since in repeated static-plan surveys, the survey is distorted when visualized in the drifter frame, we use  $e_{\text{offset}}$  as a measure of how well the survey tracks the drifter.

We compute  $g'$  by determining the centroid of the closed polygon formed by the perimeter of the survey template, as observed in the drifter frame. In Figure 15, this is given by the centroid of the polygon consisting of the vertices  $p_1' \dots p_5'$ .

We define the survey time to be the total time taken for each survey to be completed. Each completed survey is an iteration of the Lagrangian observation experiment and defines how often the AUV is able to sample the advecting water patch. A shorter survey time is therefore desirable. With AUV surge speed  $s_a$  and survey speed  $s_s$  (Section 3.3.1), from Equation (1), the survey time for the repeated static-plan surveys is given by

$$T_s = \frac{u^*}{s_a} + \frac{L_{\text{survey}}}{s_s} \tag{19}$$

where  $u^*$  is the asymptotic trailing distance of the AUV for a drifter speed  $s_d$ , derived earlier in Equation (8). Using

$u^*$  from Equation (8) in Equation (19), the survey time for repeated static-plan surveys is given by

$$T_s = L_{\text{survey}} \left( \frac{s_d}{s_s(s_a - s_d)} + \frac{1}{s_s} \right). \quad (20)$$

Survey time for transformed surveys involves a solution to Equation (17) for computation of goal waypoints for each iteration. For the following analysis, we computed the time for the transformed surveys empirically in simulation. While an analytical solution can be derived, we do not present that result in this work.

We analyzed the survey time and offset error for drifter speeds  $s_d < 1.3$  m/s in simulation for both repeated static-plan and transformed surveys. For each run of the simulation, the drifter was advected with a constant speed on a straight line while the AUV performed a box pattern using repeated static-plan and transformed surveys. Environmental perturbations and navigational errors were not emulated for this simulation. For each drifter speed, the repeated static-plan survey was run for six iterations so that the trailing distance converged. Results are shown in Figure 16 for standard AUV operational parameters, i.e. commanded AUV speed  $s_a$  of 1.5 m/s, yo-yo pitch angle  $\theta$  of  $30^\circ$  and box width  $l$  of 1 km. The survey offset error (Equation (18)) is zero throughout for the transformed surveys since by design it is implemented in the drifter frame. On the other hand, this error increases monotonically with the drifter speed, reaching  $\sim 4.9$  km at a drifter speed of 1 m/s.

The survey time is higher for repeated static-plan surveys in comparison with transformed survey plans for all drifter speeds above zero. In the case of repeated static-plan surveys, the drifter stays within the perimeter of the survey only for drifter speeds lower than **0.36** m/s. This corresponds to 70% of the observed drifter speeds in historical data and as a consequence, Lagrangian observations are not successful for 30% of the observed drifter speeds. Hence, for the five-day September 2010 Lagrangian field experiment, we used the transformed survey approach. Specifically, we used constant AUV speed in the Earth frame to utilize the optimal operational speed of the AUV at all times.

## 4. Field trials

We describe results from two field trials; a single-day deployment in June 2010 in Monterey Bay and a five-day off-shore experimentation in September 2010 with two research vessels following a drifter with an attached biogeochemical sensor. We briefly describe the experimental setup including onboard AUV autonomy followed by the description of the deployments and the results.

### 4.1. Experimental setup

Both field trials in 2010 were carried out using MBARI's Dorado AUV (Figure 17) a 4 m long propelled vehicle with a nominal speed of 1.5 m/s. Onboard autonomy is handled

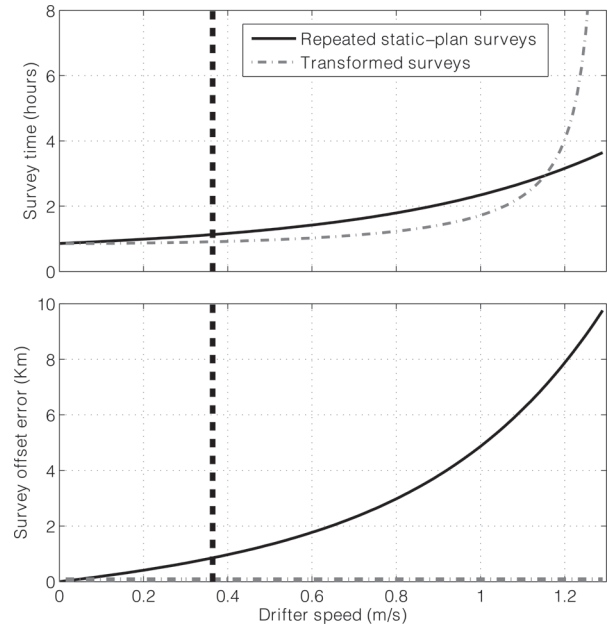


**Fig. 16.** Simulation result for survey offset error and survey time for repeated static-plan and transformed surveys using the box pattern with an edge length of 1 km. AUV surge speed of 1.5 m/s and pitch angle of  $30^\circ$  were used for this analysis. Drifter speeds between 0 m/s and 1.3 m/s was considered. The dashed vertical line shows the maximum drifter speed for which repeated static-plan surveys satisfy the enclosure criterion. Note that the survey offset error is zero throughout for the transformed survey. For transformed surveys, although the AUV can complete surveys as long as the drifter speed is less than projected AUV speed ( $\sim 1.2$  m/s), the survey time increases with increasing drifter speed, crossing 8 h for drifter speeds  $\sim 1.1$  m/s. Hence, the upper bound on drifter speed for transformed surveys depends on the operational upper bound on survey time.



**Fig. 17.** The Dorado AUV being loaded on the R/V Zephyr for the five-day off-shore drifter tracking experiment in September 2010.

using a hybrid plan-execution controller T-REX which provides a goal-directed interface to the AUV allowing a user to give high-level objectives that are resolved in situ by

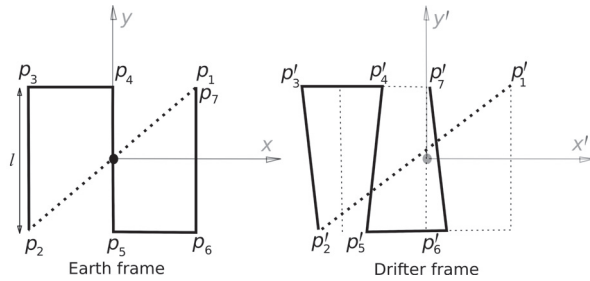


**Fig. 18.** Illustration of repeated static-plan lawnmower implemented in the June 2010 field trial. The survey is described by the waypoints  $p_1 \dots p_7$  in the Earth frame. The resulting survey in the drifter frame is described by  $p'_1 \dots p'_7$ .

the system while allowing adaptation to unexpected situations during plan execution. T-REX is built around the sense-plan-act paradigm and uses at its core a constraint-based temporal planner to synthesize plans in situ and execute these plans in the context of a dynamic environment. Re-planning occurs onboard when a partial plan has been invalidated by an unexpected situation (e.g. battery depleted faster than expected) or new objectives are injected as goals. These objectives could have been produced in situ (e.g. sensor data collected exhibit opportunistic science) or externally provided to the vehicle via a remote connection. To cope with typical planning complexity, T-REX divides the large planning problem into multiple control loops that resolve and execute their own plans within their specific functional and temporal scope. In the context of Lagrangian studies, such a goal-directed approach along with the ability to send on-the-fly new objectives in the form of drifter updates forms the basis for autonomous tracking. While the overall capability of autonomous tracking is the subject of this work, details of T-REX are outside the scope of this paper and can be found in McGann et al. (2008a,b), Py et al. (2010) and Rajan and Py (2012).

The Dorado is deployed and retrieved using the support vessel R/V *Zephyr*. A typical mission involves two AUV operations personnel along with the ship's crew. The vessel is equipped to communicate with the AUV when it is on the surface and in its vicinity via a radio link. When underwater, the vessel communicates with the AUV using an acoustic link primarily for tracking. The AUV comes with a full suite of sensors including two Seabird conductivity temperature depth (CTD) sensors, a Hobilabs 2 channel backscatter, a Teledyne ADCP, a laser optical phytoplankton counter, an ISUS nitrate sensor, a Paroscientific pressure sensor, a fluorometer for measuring colored dissolved organic matter among other instruments. For this experiment only CTD data was of relevance.

#### 4.2. June 2010 experiment: repeated static-plan surveys

This initial experiment lasted  $\sim 7$  h with repeated static-plan surveys using the lawnmower pattern carried out in

Monterey Bay, California. Figure 18 shows the lawnmower survey pattern used for this trial. The experiment was initiated with a drifter deployed at the patch center and the AUV in near vicinity. Every 10 min, the GPS-tracked drifter transmitted its location to the vessel via the Iridium satellite network. At the beginning of a survey iteration, an operator on the vessel transmitted the drifter location, course and speed to the AUV. Although this step could have been automated, it was desired to have a human in the loop for the first trial for operational safety reasons. T-REX on the vehicle computed the waypoints based on the lawnmower pattern and executed the survey. On completion of the survey, the AUV was commanded again for the next iteration by the operator on the support vessel. The AUV and drifter trajectories are shown in Figure 19.

**4.2.1. Results** The drifter experienced low speeds as shown in the histogram in Figure 20, with a mean of 0.08 m/s, and a maximum of 0.33 m/s. Hence, we were unable to validate the behavior of repeated static-plan surveys under the limiting conditions discussed earlier. Additionally, the drifter showed a sudden change in direction, undergoing a 'U-turn' within an hour (iteration 3 in Figure 19) resulting in the AUV having to travel a smaller distance to move to the initial waypoint for iteration 4. Overall, this experiment was a proof-of-concept for Lagrangian observation study and allowed us to test the communication channels between the drifter and the AUV and validate tracking and sampling of a patch for multiple iterations. The groundwork was useful in the longer experiment carried out off-shore in September 2010.

#### 4.3. September 2010 CANON experiment: transformed surveys

Based on the results of the June experiment, a five-day deployment was carried out in September 2010, 160 km off the California coast (Figure 21(a)). A specialized drifter was developed with a genomic sensor hanging 20 m below, performing in situ identification of micro-organisms (Figure 21(b)). The experiment was supported by crews on two support vessels, the R/V *Western Flyer* and the R/V *Zephyr*.

The *Flyer* visited the drifter every four hours to carry out a series of ship-based sampling experiments and lab analysis on water samples to ground-truth the drifter sensor data. The *Zephyr* was meanwhile focused on Lagrangian observation studies using the AUV. The goal was to monitor the boundary of a  $1 \text{ km} \times 1 \text{ km}$  water patch around the advecting drifter while the AUV was to perform the transformed box pattern described in Section 3.3.2 around the drifter. A number of logistical issues were kept in mind while designing and executing the experiment. Each iteration began with the latest drifter update (position and velocity) received from the drifter through an Iridium satellite link. This was transmitted to the AUV for in situ adaptation. With this input, T-REX computed the five waypoints necessary for an

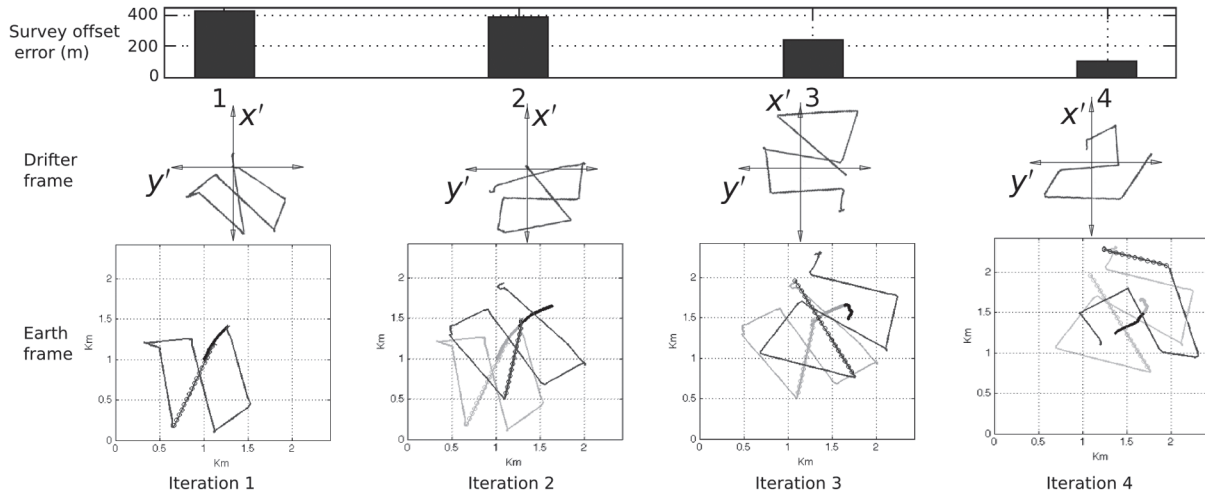


**Fig. 19.** AUV and drifter trajectories for the June 2010 drifter following experiments with the lawnmower pattern. AUV paths are shown for both the Earth frame and the drifter frame. The top plot shows the survey offset error for each iteration. The middle plot shows the drifter frame of reference for each iteration, with the location of the origin being the location of the drifter at the end of every iteration. The drifter frame is oriented in the direction of drifter advection at the end of the iteration. The AUV track is shown relative to the drifter frame through the iteration in each case. The bottom plot shows AUV and drifter tracks for each iteration in the Earth frame. For the Earth frame, an overlay of the previous iteration is included.

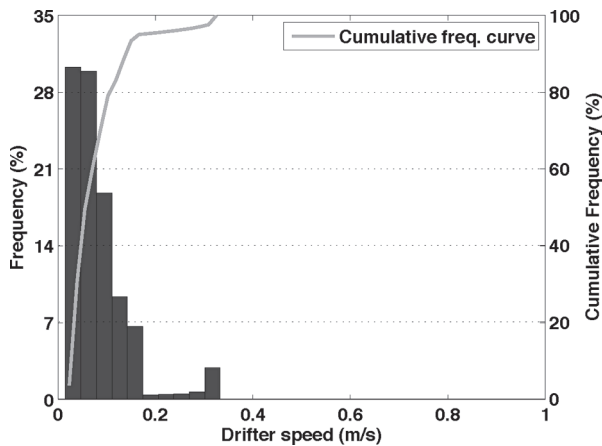


**Fig. 20.** Histogram of drifter speeds observed during the June 2010 field trial. Mean drifter speed of 0.08 m/s and a maximum drifter speed of 0.33 m/s was observed.

iteration of the box pattern using the formulation in Equation (17), with the AUV traveling at constant velocity in the Earth frame. Waypoints were computed once at the beginning of the survey with the AUV surfacing once for every survey, with each survey lasting 1–1.5 h.

**4.3.1. Results** 60 iterations were attempted over the course of five days, out of which 45 were completed successfully (some iterations had to be canceled midway or restarted due to operational reasons). Figure 22 shows the overall track lines of the drifter and the perambulating AUV over the course of the experiment. The figure shows the AUV and drifter trajectory for the five days of the experiment, with

gaps inbetween days when the AUV was being recharged. Each deployment lasted 12 hours. The black dots in the figure show the beginning of each iteration when drifter updates were received by the AUV.

During the experiment, a mean survey time of 1.2 h was observed. The survey time for each iteration depended on two factors: (a) projected drifter speed, which could vary across different iterations depending on the latest drifter speed observed and (b) the distance to the initial waypoint of the survey. This distance is dependent on how well the previous iteration is carried out, which in turn depends on various factors such as AUV localization error, drifter projection error and AUV timing error. These are discussed in Section 5.

Figure 23(a) shows the distribution of survey time. For the 45 iterations conducted, the enclosure criterion was satisfied for the true drifter for 42 iterations, and with respect to the projected drifter for 44 iterations. This corresponds to a 93.3% success for tracking the patch over the five-day field trial. Figure 24 shows the AUV path in the drifter frame for day 4 of the experiment where nine iterations of the box pattern were completed. The figure shows the desired AUV path around the drifter in the horizontal plane (1 km × 1 km square). Since each iteration was performed using the projected drifter path we show both the AUV path relative to the projected and true drifter trajectory. The paths are plotted corresponding to the origin of the drifter frame for each iteration either corresponding to the projected or the true drifter. This highlights the error in the path the AUV followed for each case, i.e. with respect to the projected drifter and true drifter path. In Section 5, we describe the sources of error with a discussion of the contribution of each to the overall quality of the surveys.

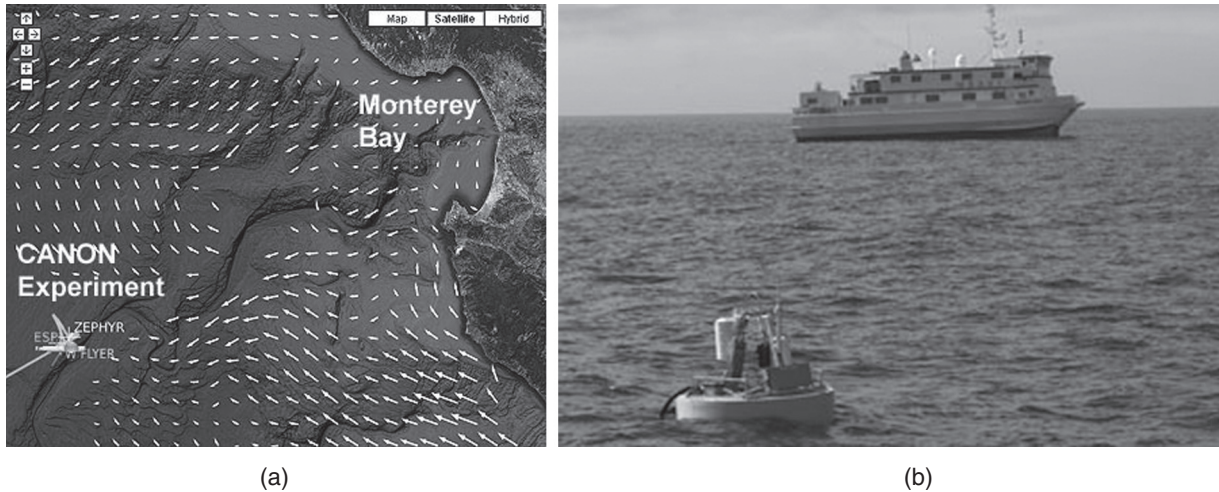


**Fig. 21.** The September 2010 CANON experiment occurred 160 km off California coast for a duration of five days. In this period, the Dorado AUV performed a Lagrangian-box survey around an GPS-tagged drifter with an attached genomic sensor: (a) location of the September 2010 CANON experiment; (b) the drifting genomic sensor in the foreground, being followed by the R/V *Western Flyer*. The AUV was monitored by a second vessel, the R/V *Zephyr*.

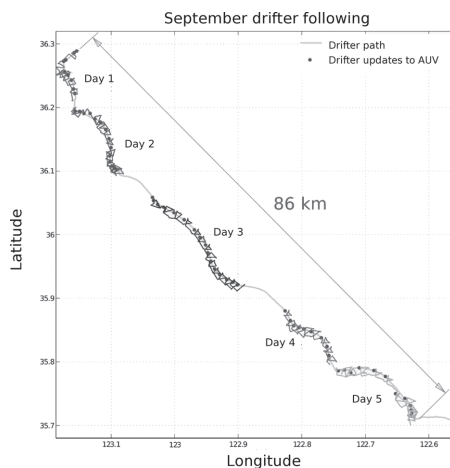


**Fig. 22.** AUV and drifter paths during the September 2010 five-day field trial. The black dots show the beginning of every iteration when the latest drifter locations were sent to the AUV. Based on these updates, the AUV computes linear projection of the drifter trajectory at the beginning of every iteration and plans waypoints in the Earth frame.

## 5. Analysis

In the previous discussion of the September field trial, we observed an error in the AUV trajectory around the drifters attributable to a number of sources. These can be from error due to the state-estimation on board the AUV and error due to the projection of the drifter trajectory during an iteration which can vary from the true trajectory of the drifter. In this section, we analyze these errors and their contribution to the quality of the surveys using two metrics: *survey offset error* and *mean surfacing error* in the drifter frame.

We start by defining the types of errors, followed by the description of the quality metrics. We then show the relationship between these errors and the survey metrics analyzed empirically, followed by a summary of the results. For the Lagrangian surveys we present in this paper, we classify the sources of error into two: intrinsic sources that result from errors in AUV state estimation and onboard planning and extrinsic sources due to logistical constraints and human-in-the-loop operation.

### 5.1. Intrinsic sources of error

The quality of surveys depends primarily on sources of error inherent in AUV operations and the assumptions made in the design of the survey. The former is due to the state-estimation performed onboard the AUV which provides it with an estimate of its current location and velocity. The latter is the assumption we make about the drifter trajectory during an iteration, namely that the drifter will continue to travel in a straight line with the speed and in the direction computed from the last two position updates. We will now discuss these two error sources.

**5.1.1. State-estimation error** AUVs suffer from localization errors due to environmental perturbations such as sub-surface currents and constraints on obtaining absolute position measurements. Since GPS location fixes are not available underwater, AUVs surface at regular intervals (every 20–30 min for the Dorado). While frequent GPS-fixes are essential to reduce the navigational error, multiple yo-yos are usually performed before surfacing. This is done to ensure continuous recording of scientific data as well as to minimize surface time especially in high-traffic areas. When underwater, the AUV dead-reckons using its

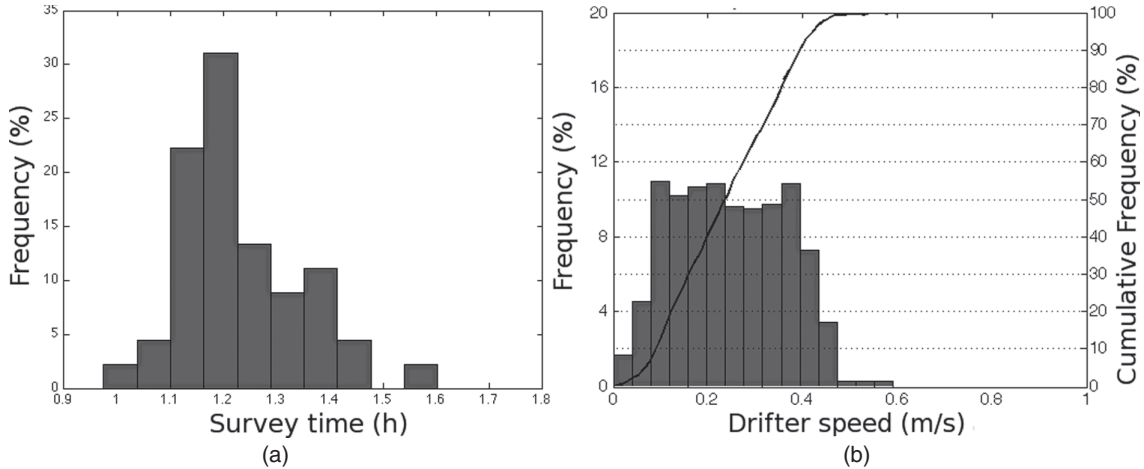


**Fig. 23.** Drifter speed and survey time statistics for the September field experiment. Mean drifter speed of 0.245 m/s and maximum speed of 0.6 m/s was observed during the five-day experiment: (a) distribution of survey time for the 45 iterations of the field trial; (b) distribution of drifter speeds during the five days of the experiment.

depth sensor, onboard compass and inertial navigation system (INS). The accumulated position error between surfacings can be up to 500 m for 30 min. During the September field trial, a median surfacing error of 220 m was observed for the goal waypoints in the Earth frame. For our work, AUV state-estimation error affects Lagrangian surveys in two ways: surfacing error in the Earth frame and timing errors.

Figure 25 illustrates how the AUV navigates to a goal waypoint. In this figure, the AUV is at location  $p_1$  at time  $t_1$  and is tasked to navigate to goal location  $p_2$  at time  $t_2$ . Dorado's onboard controller performs straight-line navigation between commanded waypoints (as projected on the horizontal plane) at constant speed. The controller considers the goal reached when the AUV has crossed a 'completion line' through the goal location, perpendicular to the AUV's direction of travel. Given the goal location and time, the controller computes and executes its parameters of traversal (surge speed, pitch angle, heading) targeting to surface when the goal waypoint is reached. The nature of the AUV controller makes it explicitly target reaching the goal location, with no guarantees on the time of arrival at the location. Based on the state estimator output and the onboard controller, the AUV could surface at time  $t_{21}$  at location  $p_{21}$ , with the belief that the goal  $p_2$  has been reached. However, there could be a large error in the surfacing location and the goal location. As a result the AUV attempts to correct its course to finally reach the waypoint, accumulating some error in surfacing, but a significant error in its timing.

Consider an iteration from the September experiment shown in Figure 26. It shows the AUV path in Earth and drifter frames, along with the actual drifter and projected drifter path. The planner on board the AUV computes its trajectory in the form of five waypoints corresponding to the corners of the survey, along with the arrival times at

those waypoints. This trajectory in the Earth frame corresponds to the desired survey template being implemented in the drifter frames. To measure the error due to the two factors discussed above, we use the following error metrics for each iteration of a survey: (a) the mean surfacing error in the Earth frame (MSE-EF) and (b) the mean timing error (MTE). The former captures mean error in surfacing for the five waypoints in the Earth frame while the latter captures the mean error in the time of arrival for these five waypoints. If  $(p_1, t_1) \dots (p_5, t_5)$  are the desired waypoints and times of arrival for the five waypoints in the Earth frame for an iteration of the survey and the AUV achieves  $(p_1^*, t_1^*) \dots (p_5^*, t_5^*)$ , then the mean surfacing error in Earth frame (or MSE-EF) is given by

$$e_{\text{MSE-EF}} = \frac{1}{5} \sum_{i=1}^5 |p_i - p_i^*|. \quad (21)$$

The mean timing error is similarly given by

$$e_{\text{MTE}} = \frac{1}{5} \sum_{i=1}^5 (t_i - t_i^*). \quad (22)$$

**5.1.2. Drifter trajectory projection error** For each iteration of our experiment, we estimate the latest observed drifter velocity and the linearly projected drifter trajectory assuming constant velocity for the duration. Changes in drifter speed and course during an iteration results in the true drifter trajectory being different from the AUV's projection. This can be observed in Figure 26 where we can see the difference between the linear projection of the drifter path and the true drifter path in the Earth frame. The path-plan for the AUV is designed for the projected trajectory of the drifter resulting in an error in the drifter-frame survey with respect to the true trajectory of the drifter. We measure this error as the distance between the final projected drifter location and

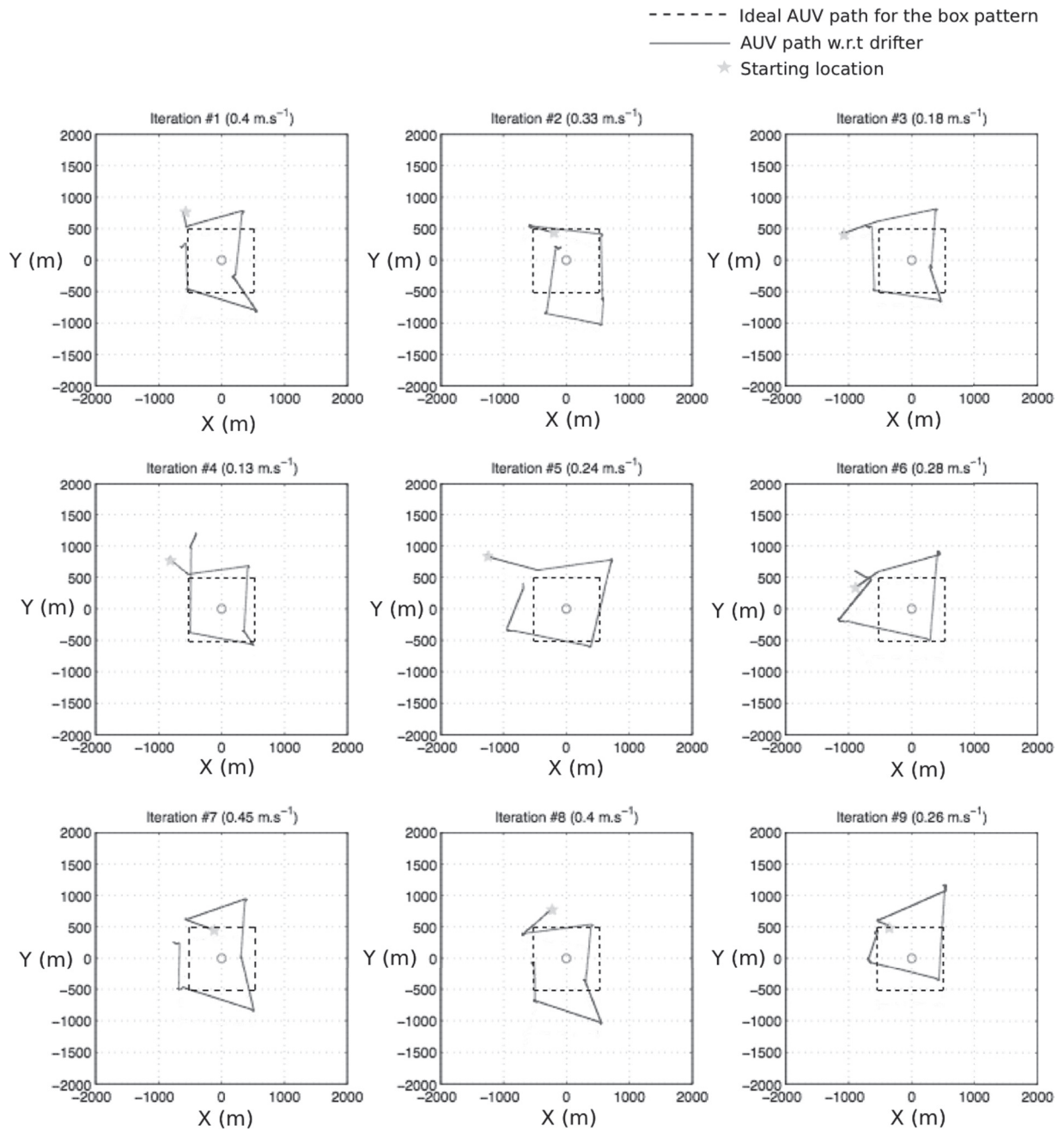


**Fig. 24.** Iterations from day 4 of the September trial illustrating the drifter frame views of the AUV path. In total, nine iterations were conducted that day. Each of the plots shows the desired AUV trajectory (square with dotted edges with length 1000 m). The star shows the starting location of the AUV for each iteration, and the AUV path relative to the drifter is shown with a solid line.

the true drifter location at the end of every iteration and call it the *drifter projection error*.

### 5.2. Extrinsic sources of errors

Some errors can be attributed to operational choices. During complex field campaigns, many platforms exist in close proximity for an extended period of time. Experiment design decisions are consequently made to reduce operational hazards and chance of equipment damage (e.g.

AUV collisions with the vessel hull due to improper surfacings). Although the communication channels were set up to be fully-automated, human-in-the-loop operation was desired to ensure: (a) situational awareness among operations personnel and (b) validation of plans to avoid errors due to environmental perturbations not accounted for in experiment design such as excessive drifter speeds, strong sub-surface currents, and error in drifter position data. The impact of human decision-making was kept to a minimum; an additional check was added before onboard planning

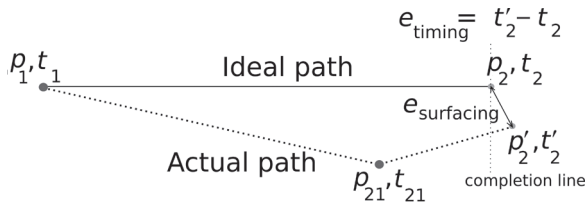


**Fig. 25.** Illustration of AUV position and timing error. Since the AUV dead-reckons when underwater, with corrections from GPS only when it surfaces (every  $\sim 30$  min), it can experience substantial localization errors. This figure shows a scenario where the AUV surfaces ahead of its goal waypoint and compensates for the error, finally surfacing near the goal waypoint with both positional and timing error.

was initiated at the beginning of a survey. Also, to ensure the ship's crew were cognizant of where the AUV might surface, waypoints were not recomputed after initial generation. AUV plans therefore were not adaptive during an iteration even if the onboard capability existed. The key extrinsic sources of errors were as follows:

**Lag in drifter position update:** during the experiment, there was a lag of  $\sim 15$  min for drifter location data sent to the AUV. This delay was due both to the update rate via the communication network from the drifter ( $\sim 10$  min) as well as operational delays due to human in-the-loop commanding for safety.

**Wait time at surface while acquiring GPS fix:** additional delays adding up to imprecise drifter speeds being fed to the AUV occurred because the AUV itself required up to two min to obtain a GPS fix when on the surface. During this period, the AUV is drifting in the Earth frame, resulting in errors in survey plans which were implemented in the drifter frame.

**Distance to first waypoint of an iteration:** in the transformed-survey approach, we make the assumption that the last waypoint of one iteration is coincident with the first waypoint of the next iteration. However, since the waypoints are planned based on the linear projection of the latest drifter velocity, there is always a residual distance between where one iteration ends and the next should begin. We do not, however, compensate for this error in our survey plan which results in a timing error in starting the iteration.

### 5.3. Survey quality metrics

To evaluate the quality of our surveys, we use two metrics: the survey offset error and the mean surfacing error of the AUV in the drifter frame. The survey offset error (defined in Section 3.4) is a measure of how close the center of the transformed survey is to the origin of the drifter frame. The smaller the survey offset error the better, zero being the ideal case. Figure 27 shows the distribution of survey offset

error for the 45 iterations of the September field trial. The mean error was 282 m and the maximum 1075 m. For three of the 45 iterations, the enclosure criterion was not satisfied and these corresponded to the top three survey offset errors of 1075 m, 793 m and 734 m respectively. By definition, iterations with high survey offset error are prone to a non-satisfying enclosure criterion.

The mean surfacing error in the drifter frame or the MSE-DF is a measure of how close the geometry of the survey is to that of the desired survey pattern. If the implemented survey is highly distorted due to errors in the experiment, for example because of the AUV surfacing far away from intended waypoints, then the MSE-DF will be high. If  $(p''_1, t''_1) \dots (p''_5, t''_5)$  are the desired waypoints and times of arrival for the five waypoints in the Earth frame for an iteration of the survey and the AUV achieves  $(p''^*_1, t''^*_1) \dots (p''^*_5, t''^*_5)$ , then the MSE-DF is given by

$$e_{\text{MSE-DF}} = \frac{1}{5} \sum_{i=1}^5 |p''_i - p''^*_i|. \quad (23)$$

Figure 28 shows the distributions of the surfacing error in the Earth frame, the surfacing error in drifter frame, and the timing error for the iterations of the September field trial.

### 5.4. Analysis of the September trial results

We analyzed which sources of error contributed the most to the quality of surveys during the September field trial using the quality metrics and the intrinsic errors described earlier. Our goal was to determine the contribution of the various sources of error (MSE-EF, MTE and drifter projection error) to the overall quality of the survey measured using the MSE-DF and the survey offset error. The MSE-DF captures the effect of distortion of the survey, whereas the survey offset error captures the distance between the implemented patch center, and the desired the patch center (the drifter location). We look at the correlation of various error terms with these two metrics. For the 45 iterations from September, the MSE-EF and MTE were computed using Equations (21) and (22) respectively. The quality metrics, survey offset error and the MSE-DF were computed using Equations (23) and (18) respectively. The first two contributions are measured with the MSE-DF metric. It correlates most with the MSE-EF, with a correlation coefficient  $R = 0.62$ . The MSE-DF is correlated with the MTE with  $R = 0.56$ . We also analyzed the correlation between the error terms themselves; the MSE-EF being correlated to the MTE with  $R = 0.33$ . As mentioned earlier, survey offset error is used as a measure of the survey quality with regard to the true drifter trajectory. It is correlated with the drifter projection error with  $R = 0.60$ , to the MTE with  $R = 0.25$  and to the MSE-EF with  $R = 0.15$ . Hence, the survey offset error is affected the most by our assumption of a linear-drifter trajectory projection. Figure 29 shows the correlation coefficient between the MTE and MSE-DF,

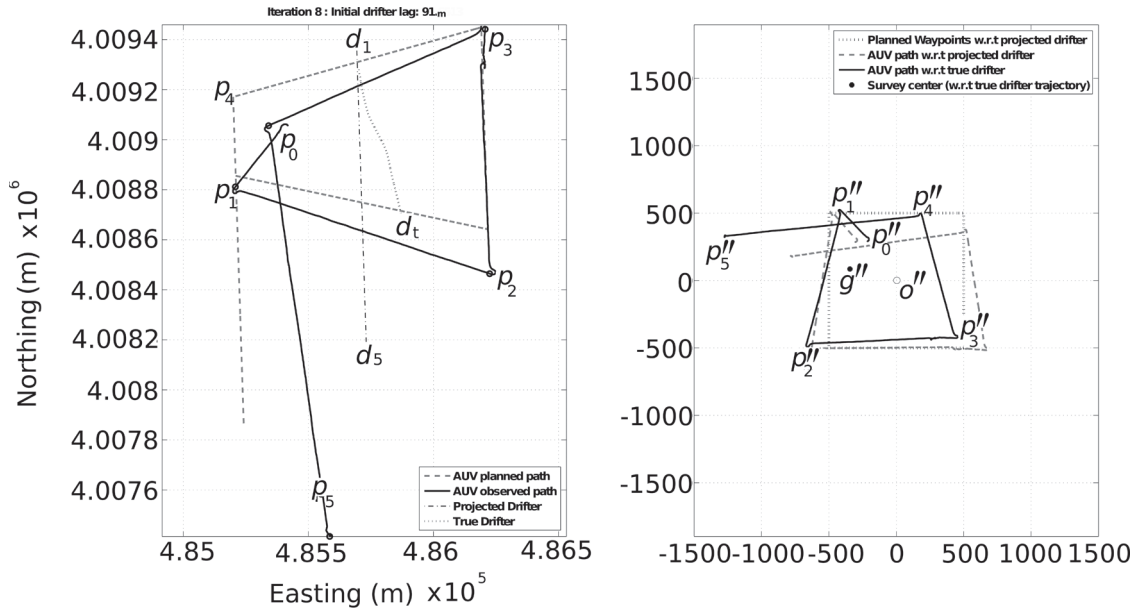


**Fig. 26.** The Earth frame (left plot), showing planned and observed AUV paths and the Drifter frame (right plot) showing the observed AUV path relative to the true drifter and observed AUV path relative to the projected drifter. In the Earth frame,  $p_1 \dots p_5$  are the locations where the AUV surfaced.  $p_0$  shows the location of the AUV at the beginning of the survey iteration. Thus, the AUV has to initially travel to the first waypoint  $p_1$  before beginning the survey iteration, resulting in additional error in the survey quality. The drifter was located at  $d_1$  in the beginning of the survey iteration. The projected location of the drifter at the end of the iteration is  $d_5$ , whereas the true location is  $d_t$ . In the drifter frame, the corresponding surfacings of the AUV are at  $p''_1 \dots p''_5$ , and the survey center is at  $g''$ .

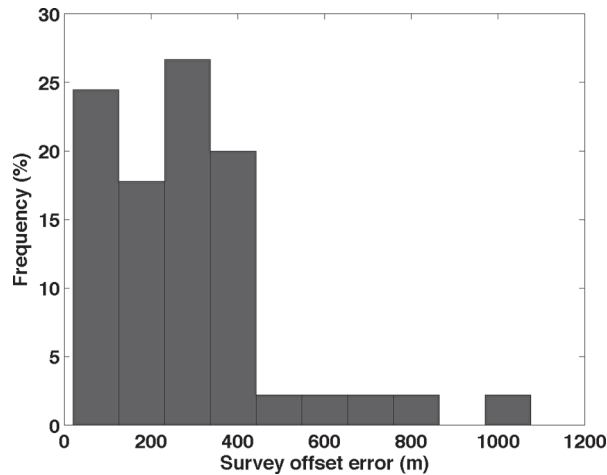


**Fig. 27.** Distribution of survey offset error for the 45 iterations of the September field trial. The mean error was 282 m, and maximum error of 1075 m (corresponding to one of the three iterations where the enclosure criterion was not satisfied).

the MSE-EF and MSE-DF, the MTE and MSE-EF and the drifter projection error and survey offset error.

We summarize by drawing two conclusions from the above analysis. First, since the survey offset error is most strongly correlated to the drifter projection error, by improving the projection method, we hope to improve the overall accuracy of our experiments. Second, MSE-DF, which is a measure of the error in survey quality purely

due to the effect of AUV localization error<sup>4</sup> is correlated to both the MSE-EF and the timing error as expected. This is the inherent error in tracking the drifter due to the state-estimation error of the AUV. Hence, with better state-estimation and with a reduction of the AUV localization error, we can improve how the AUV implements the desired survey pattern in the drifter frame.

### 6. Conclusions and future work

In this paper, we have demonstrated methodologies to observe advecting oceanographic features with an autonomous underwater vehicle and a GPS-tracked drifter. The drifter was used to tag a feature (or water patch) of interest and the AUV was used to survey the patch using various survey patterns. We propose two approaches: (a) repeating static-plan surveys and (b) transformed surveys where the planning is done in the drifter (or patch) frame of reference. A series of field trials were conducted targeting the two approaches.

The work provides marine scientists with an approach to observe and understand microbial evolution within an advecting mass of water, characterizing a feature of interest. We started by extending current static-plan surveys that allow tracking of a drifter by repositioning the AUV to the latest drifter location at the end of every survey. An enclosure criterion was specified as the constraint necessary for successful tracking of a tagged patch. We derive the upper limit on the drifter (or patch) speed for which this

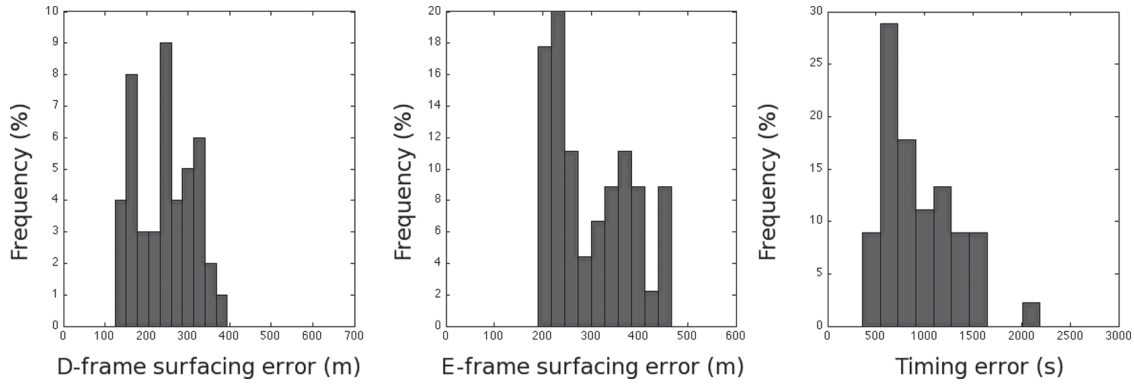


Fig. 28. Descriptive statistics for timing and surfacing errors in the drifter and Earth frames.

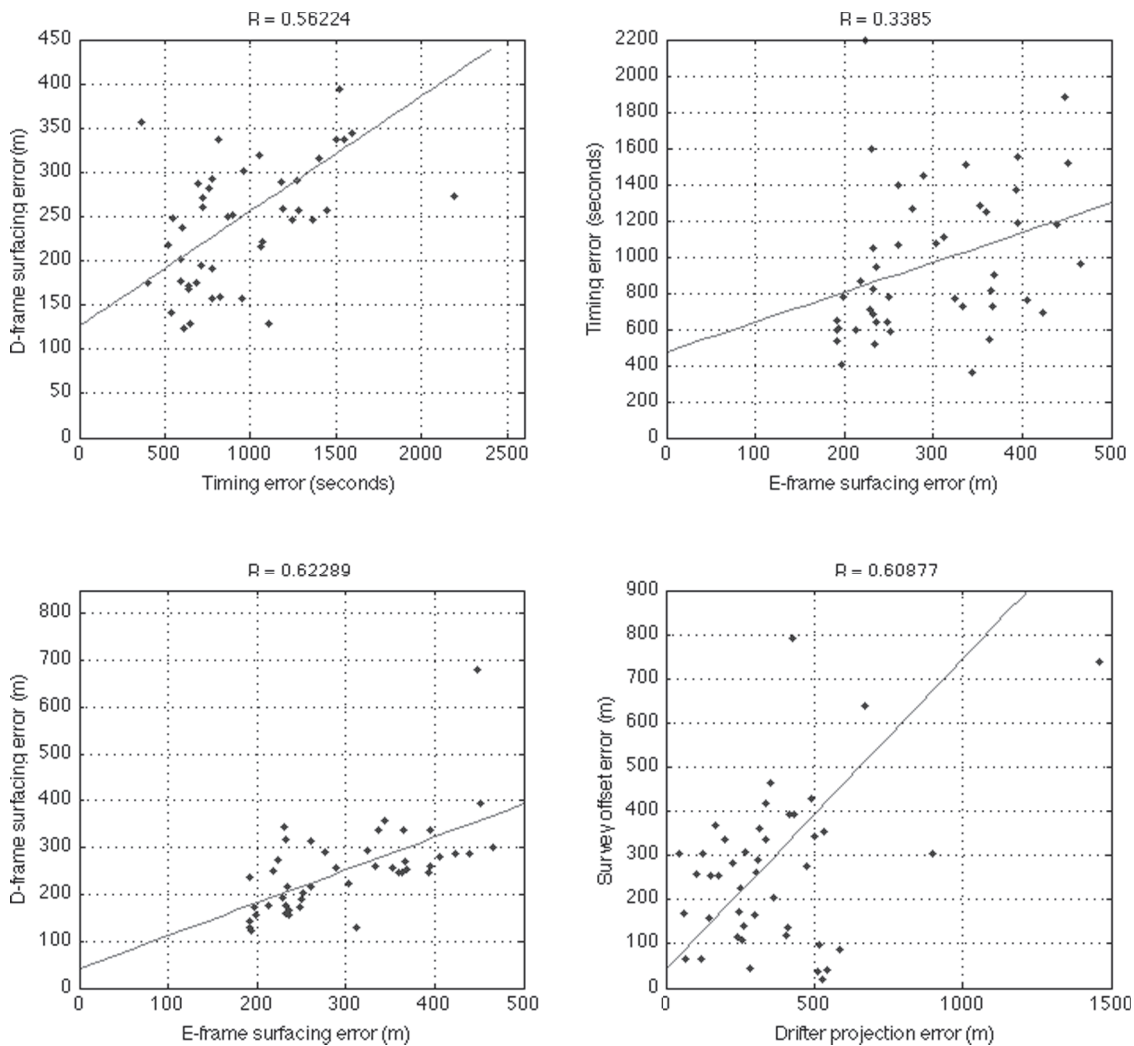


Fig. 29. Scatter plots for error-pairs along with the correlation coefficient  $R$ .

criterion is satisfied for repeated static plan surveys by an autonomous robot.

We define quality metrics that allow us to evaluate the performance of our approach. Simulations are carried out to

compare the performance of repeated static plan and transformed surveys. Through these simulations, we show that transformed surveys are ideal for Lagrangian observation studies with an AUV. Our method was validated in a

five-day off-shore field trial where the AUV successfully tracked and sampled the patch of water tagged by a drifter. During this period, 45 iterations were carried out, each lasting for more than an hour and the enclosure criterion was satisfied 93.3% of the time (42 iterations).

The novelty of our work is four-fold; first, we show that there are limitations in using extensions of static surveys repeatedly repositioned with the advecting patch. Second, we quantitatively derive an envelope on the speeds of patches that can be tracked autonomously. Third, we provide important ways to measure the performance of such surveys analytically. Finally, we demonstrate the concept of autonomous Lagrangian experiments in the field with an inter-disciplinary team.

An important lesson learned for Lagrangian studies from this work is that, by ensuring a desired template is implemented in the drifter frame of reference, one can ensure that an autonomous platform is able to track a drifting patch continuously. This work therefore, provides the empirical basis of tracking the ecological life-cycles of water patches with significant biological activity, where acquiring measurements at sufficient spatial and temporal resolution is important.

To the best of our knowledge, our work presents the first set of experiments where Lagrangian observation studies were carried out with an autonomous platform successfully tracking a patch of water successfully.

We are now working on multiple areas to improve both the approach and the validating experiments. First, to increase the level of autonomy by enabling the AUV to receive drifter locations directly to plan each iteration; one consideration is to ensure that the experiment occurs sufficiently off-shore to discount any possibility of drifting towards shallow waters; preliminary results in near-shore CANON experiments in 2011 have been encouraging thus far. Second, we want to address the effect of linear drifter trajectory projection for each iteration by considering more refined surveys where the AUV is able to compensate for drifter locations during the survey. Finally, we propose to study non-deterministic approaches to drifter projection and modeling, those that can be embedded within an autonomous platform. Doing so will add an entirely new capability to observe and understand the ecological life cycle in the upper water-column of the ocean.

## Notes

1. Oxygen depleted regions in the ocean.
2. From (Rudnick and Perry 2003): The terms *Lagrangian* and *Eulerian* describe different frames of reference for specifying or observing fluid properties. An Eulerian specification of a fluid property is a function of space and time. The Eulerian frame of reference is probably most familiar to people; we stand on the shore and watch the river flow by us. A Lagrangian specification is a function of an identifiable piece of fluid and time. The Lagrangian frame of reference moves with the fluid; we sit in an inner tube and float down the river.
3. The horizontal transport of a patch of water.
4. Note that for this error metric, we perform our computation relative to the projected drifter.

## Funding

This work was supported by the NOAA MERHAB program (grant number NA05NOS4781228) and by the NSF (grant numbers CCR-0120778, CNS-0520305 and CNS-0540420) by the ONR MURI program (grant numbers N00014-09-1-1031 and N00014-08-1-0693), by the ONR SoA program, and by a gift from the Okawa Foundation. MBARI authors are funded by a block grant from the David and Lucile Packard Foundation.

## Acknowledgements

We would like to thank Geoff Hollinger (USC) and Ryan Smith (QUT) for their valuable comments on an earlier draft of the paper. We acknowledge the extensive feedback provided by the anonymous reviewers which have substantially strengthened the paper. Finally, we thank our colleagues in the CANON program and the crew of the R/V *Zephyr* for supporting our work at MBARI.

## References

- Anderson D, Hoagland P, Kaoru Y and White A (2000) Economic impacts from harmful algal blooms (HABs) in the United States. Technical report, Woods Hole Oceanographic Institution, USA.
- Bellingham JG and Willcox JS (1996) Optimizing AUV oceanographic surveys. In: *1996 symposium on autonomous underwater vehicle technology (AUV '96)*, Monterey, USA, 2–6 June 1996, pp. 391–398. Washington DC: IEEE Computer Society.
- Controlled, agile and novel observing network (CANON) (2010). Available at: <http://www.mbari.org/canon/>.
- Chavez FP et al. (1997) Moorings and drifters for real-time interdisciplinary oceanography. *Journal of Atmospheric and Oceanic Technology* 14(5): 1199–1211.
- Davis RE (1985) Drifter observations of coastal surface currents during CODE: the method and descriptive view. *Journal of Geophysical Research* 90: 4741–4755.
- Fiorelli E et al. (2006) Multi-AUV control and adaptive sampling in Monterey Bay. *IEEE Journal of Oceanic Engineering* 31(4): 935–948.
- Franchi A, Stegagno P, Rocco MDD and Oriolo G (2010) Distributed target localization and encircling with a multi-robot system. In: *7th IFAC symposium on intelligent autonomous vehicles (IAV 2010)*, Lecce, Italy, 6–8 September 2010.
- Frew EW and Lawrence D (2005) Cooperative stand-off tracking of moving targets by a team of autonomous aircraft. In: *AIAA guidance, navigation, and control conference*, San Francisco, USA, 15–18 August 2005, pp. 4885–4895. Reston: American Institute of Aeronautics and Astronautics.
- Hu Z, Petrenko A, Doglioli A and Dekeyser I (2011) Study of a Mesoscale anticyclonic eddy in the Western part of the Gulf of Lion. *Journal of Marine Systems* 88(1): 3–11.
- Kimball P and Rock S (2010) Sonar-based iceberg-relative navigation for autonomous underwater vehicles. *Deep Sea Research Part II: Topical Studies in Oceanography* 58: 1301–1310.

- Lumpkin R and Pazos M (2007) Measuring surface currents with surface velocity program drifters: the instruments, its data and some recent results. In: Griffa A, Kirwan Jr AD, Mariano AJ, Özgökmen T and Rossby HT (eds) *Lagrangian Analysis and Prediction of Coastal and Ocean Dynamics*. Cambridge: Cambridge University Press.
- Mas I, Li S, Acain J and Kitts C (2009) Entrapment/escorting and patrolling missions in multi-robot cluster space control. In: *2009 IEEE/RSJ international conference on intelligent robots and systems (IROS '09)*, St. Louis, USA, 10–15 October 2009, pp. 5855–5861. Piscataway: IEEE Press.
- McGann C, Py F, Rajan K, Ryan JP and Henthorn R (2008a). Adaptive control for autonomous underwater vehicles. In: Fox D and Gomes CP (eds), *Proceedings of the 23rd AAAI Conference on Artificial Intelligence*, pp. 1319–1324. AAAI Press.
- McGann C, Py F, Rajan K, Thomas H, Henthorn R, and McEwen RS (2008b) A deliberative architecture for AUV control. In: *IEEE International Conference on Robotics and Automation*, pp. 1049–1054.
- Molcard A, Piterberg LI, Griffa A, Ozgokmen TM and Mariano A (2003) Assimilation of drifter observations for the reconstruction of the Eulerian circulation field. *Journal of Geophysical Research* 108: 3056.
- Py F, Rajan K and McGann C (2010) A systematic agent framework for situated autonomous systems. In: *9th international conference on autonomous agents and multiagent systems*, Toronto, Canada, 10–14 May 2010, vol. 2, pp. 583–590. Richmond: IFAAMAS.
- Rajan K and Py F (2012) T-REX: partitioned inference for AUV mission control. In: Roberts GN and Sutton R (eds) *Further Advances in Unmanned Marine Vehicles*. Stevenage: IET.
- Rudnick DL and Perry MJ (2003) ALPS: autonomous and Lagrangian platforms and sensors. Report. Available at: <http://www.geo-prose.com/ALPS>.
- Ryan JP et al. (2005) Coastal ocean physics and red tides: an example from Monterey Bay, California. *Oceanography* 18: 246–255.
- Salman H, Jones C and Ide K (2008) Using flow geometry for drifter deployment in Lagrangian data assimilation. *Tellus, Series A: Dynamic Meteorology and Oceanography* 60: 321–335.
- Saripalli S and Sukhatme GS (2003) Landing on a moving target using an autonomous helicopter. In: *4th international conference on field and service robotics (FSR 2003)*, Mt. Fuji, Japan, 14–16 July 2003.
- Sciavicco L, Sciavicco L and Siciliano B (2000) *Modelling and Control of Robot Manipulators*. Berlin: Springer-Verlag.
- Smith RN, Chao Y, Li PP, Caron DA, Jones BH, and Sukhatme GS (2010a) Planning and implementing trajectories for autonomous underwater vehicles to track evolving ocean processes based on predictions from a regional ocean model. *International Journal of Robotics Research*, 26(12).
- Smith RN, Pereira AA, Chao Y, Li PP, Caron DA, Jones BH and Sukhatme GS (2010b) Autonomous underwater vehicle trajectory design coupled with predictive ocean models: A case study. In: *IEEE International Conference on Robotics and Automation*, pp. 4770–4777.
- Surface temperature experimental longitude latitude asset (STELLA) drifter project (2006). Available at: <http://www.mbari.org/bog/drifterdata/>.
- Willcox JS, Bellingham JG, Zhang Y and Baggeroer AB (2001) Performance metrics of oceanographic surveys with autonomous underwater vehicles. *IEEE Journal of Oceanic Engineering* 26(4): 711–725.
- Zhang F, Fratantoni DM, Paley D, Lund J and Leonard NE (2007) Control of coordinated patterns for ocean sampling. *International Journal of Control* 80(7): 1186–1199.